



Very High Cycle Fatigue (VHCF) of notched specimens: a review

Paolo Zuliani, Carlo Boursier Niutta, Davide Salvatore Paolino, Andrea Tridello

Politecnico di Torino, Department of Mechanical and Aerospace Engineering, Torino, 10129, Italy

paolo.zuliani@studenti.polito.it, carlo.boursier@polito.it, davide.paolino@studenti.polito.it, andrea.tridello@studenti.polito.it

Filippo Berto

Department of Chemical Engineering, Materials and Environment, Università La Sapienza, 00185, Roma, Italy

filippo.berto@uniroma1.it



Citation: Zuliani, P., Boursier Niutta, C., Paolino, D.S., Berto, F., Tridello, A., Very High Cycle Fatigue (VHCF) of notched specimens: a review, *Fracture and Structural Integrity*, 74 (2025) 385-414.

Received: 03.08.2025

Accepted: 02.09.2025

Published: 13.09.2025

Issue: 10.2025

Copyright: © 2025 This is an open access article under the terms of the CC-BY 4.0, which permits unrestricted use, distribution, and reproduction in any medium, provided the original author and source are credited.

KEYWORDS. Very High Cycle Fatigue, Notch effect, Ultrasonic fatigue testing.

INTRODUCTION

In the last years, research on the Very High Cycle Fatigue (VHCF) or gigacycle fatigue response of materials has received significant attention in the academic community and among industries. This can be mainly attributed to the continuous increase in demand for components with high fatigue performances, i.e., components with expected life beyond the current standard and significantly exceeding the conventional $2 \cdot 10^6$ cycles. A clear example is represented by automotive and aerospace components [1,2]. One of the main peculiarities of failures in the VHCF region is the failure mode: indeed, in the HCF life region, failures mainly originate from the specimen surface, whereas manufacturing and microstructural defects are the weakest sites where a crack forms when low amplitude loads are applied for a very high number of cycles [3]. Therefore, models and theories developed to deal with the fatigue response in the High Cycle Fatigue (HCF) regime should be experimentally verified to prove their validity even in the VHCF life region.

For example, the experimental assessment of the notch effect has to deal with issues that are not present when carrying out conventional tests. For example, the majority of fatigue tests investigating the VHCF life region are carried out by using the ultrasonic testing machine, working in resonance conditions and applying a loading frequency of 20 kHz. The tested specimens are designed to meet the axial resonance conditions in a range close to 20 kHz, and this controls the stress distribution. Accordingly, the design of specimens for ultrasonic fatigue tests can be complex, as well as the definition of a



stress concentration factor for a specimen with a notch, since, for the same geometry, the stress distribution and the resulting K_t can be different from that for a specimen to be tested with conventional testing machine [4–7]. Similarly, failure modes are different in VHCF, mainly originating from defects rather than the specimen surface. Accordingly, the interaction between defects and the complex stress distribution close to the notch plays a significant role [6,7]. Additionally, the local increase of the stress may cause a change of failure modes [4,8–11]. Due to this, the notch sensitivity in the VHCF regime is different with respect to the HCF regime. These examples highlight the importance of investigating the notch effect in the VHCF life region and the complexity of this phenomenon, which should be thoroughly experimentally investigated, since a safe design against VHCF of parts with geometrical discontinuities failure cannot rely on the results obtained in the High Cycle Fatigue region.

In the present work, a review on the influence of notch and geometric discontinuities on the Very High Cycle Fatigue (VHCF) response of metallic materials is carried out. Experimental results on notch effect available in the literature have been critically analyzed and reviewed. The primary objective of this work is to organize literature findings, to provide the reader with general trends, useful for the design against VHCF failures of parts with notches. The strengths and weaknesses of the available approaches are discussed, providing a guidance for future research and highlighting the current gap of knowledge.

VERY HIGH CYCLE FATIGUE OF NOTCHED SPECIMENS

In this section, the results reported in the literature are presented in detail. Particularly, the following aspects will be discussed for each article:

- 1) **The failure mechanism.** According to Mugarabi [12] metallic materials in the VHCF fatigue can be divided into two categories: “Type I” and “Type II”. The first type of material (such as low carbon steel) is characterised by homogeneous microstructure and usually shows a fracture nucleated at the surface in all the fatigue life. The second type (i.e. high-strength steels and titanium alloys) usually fails from cracks nucleated from internal defects because their VHCF behaviour is highly influenced by the presence of pores, non-metallic inclusions and secondary phase. However, the presence of a notch can cause a local increase of the stresses that leads to surface crack initiation also in “Type II” materials.
- 2) **The loading frequency.** In order to test materials in the VHCF regime, fatigue tests are mostly carried out at ultrasonic loading frequency (20 kHz). According to Hong et al. [13], even if the temperature increase is controlled, a strain rate effect could be present. Particularly, the materials which have a high sensitivity to the loading frequency are low-strength metallic materials (i.e. structural steels) and materials with a BCC lattice. Materials that have HCP lattice (titanium alloys), FCC lattice (aluminium alloys) and high-strength metallic materials, have a low sensitivity to the loading frequency.
- 3) **The stress concentration around the notch.** While for fatigue test in the HCF regime the static stress concentration factor can describe the stress concentrations accurately for a defined specimen and part geometry, this is not always true when the tests are carried out at ultrasonic frequency because the stress distribution is governed by the elastic wave theory. Consequently, the approach used by each author to quantify this effect will be discussed in each section.
- 4) **The notch effect.** The notch effect may not be constant within the VHCF life range and this will be discussed and investigated in the paper. The notch effect refers to the phenomenon of fatigue strength reduction due to the presence of a notch. To quantify this effect, two properties are typically used in literature:
 - a) The notch fatigue factor (K_f), which is the ratio of the fatigue strength of unnotched specimens (σ_a^{smooth}) to fatigue strength of notched specimens ($\sigma_a^{notched}$).

$$K_f = \frac{\sigma_a^{smooth}}{\sigma_a^{notched}} \tag{1}$$

- b) The notch sensitivity (q), which correlates (K_f) with the stress concentration factor (K_t) with equation equation

$$q = \frac{K_f - 1}{K_t - 1} \tag{2}$$

In this article, the notch effect is discussed for each scrutinized study using the notch fatigue factor (K_f). To classify the different articles, different criteria can be considered: the type of fatigue test (conventional fatigue testing or ultrasonic fatigue testing), the material or the manufacturing process (conventional process or Additive Manufacturing

process). Since there are only a few articles on specimens produced by AM and most of the articles are carried out at ultrasonic frequency, the articles have been classified by considering the material type. In authors' opinion, this is the best and clearest classification to discuss notch effect by considering the available literature results. Fig. 1 shows that there are eight articles on steels, four on aluminium alloys, three on titanium alloys, and only one on an INCONEL superalloy. As a consequence, the section dedicated to the INCONEL alloy has been included in the same chapter as the titanium alloys, under the title "Other Metallic Materials".

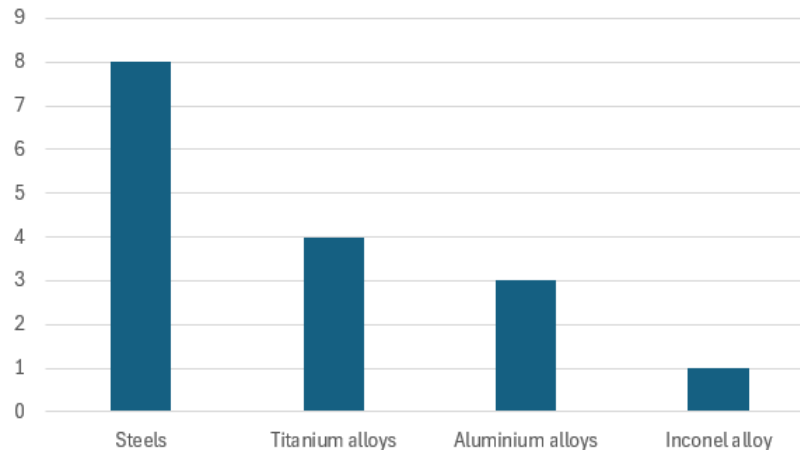


Figure 1: Published articles for each material type about the notch effect in the VHCF fatigue.

Steels

The first article about the notch effect in the VHCF cycle regime was published by Akiniwa et. al. [8] and it investigates the notch sensitivity of a bearing steel. The authors have analysed the fatigue behaviour of two different batches of SUJ2 bearing steel (100 Cr6). Both of them were normalised, quenched, tempered and polished with emery paper. The difference is that the first batch was also electro-polished to remove residual stresses (type A), while the second one was not electro-polished (type B). The fatigue tests were all conducted at 20 kHz with a stress ratio of $R=-1$. The analysis has been conducted using different geometries: smooth, circumferentially notched (Fig. 2(a)) and drill hole (Fig. 2(b)) The first geometry was tested using both type A and type B materials.

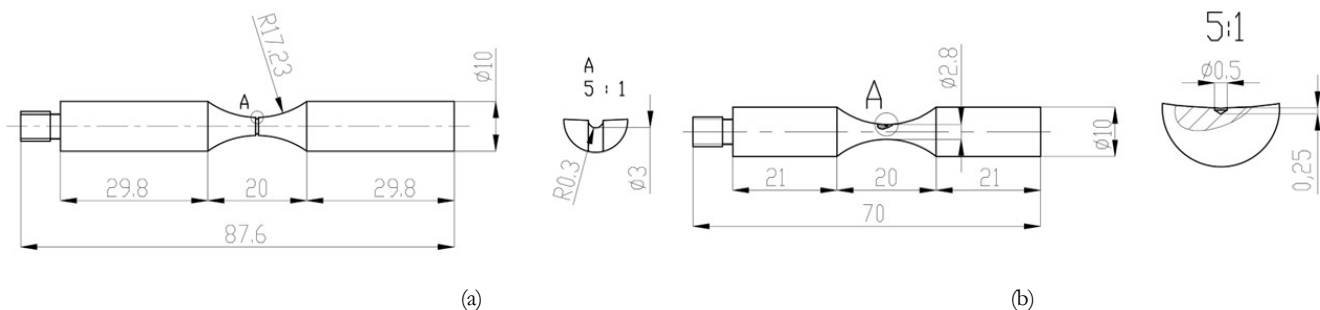


Figure 2: Geometries of the specimens used by [8]: (a) notched specimens (b) drill hole specimens.

The Scanning Electron Microscopy (SEM) showed that the type A specimens broke mainly near the surface, while type B specimens failed by internal defects. Different behaviour has been attributed to the presence of compressive residual stresses in type B specimens. On the contrary, for all notched and drill-hole specimens the fracture started near the surface because the stress in this point is high and because only type A material was used. One important result of this study is that the notch fatigue factor K_f shows a big decrease with the increase of the number of cycles. In particular, the circumferentially notched specimens show a reduction of -5.5 %, while the drill holed the reduction is -1.47 %. The different sensitivity to the number of cycles is schematically represented in Fig. 3(a), while the experimental results digitized from [8] are reported in Fig. 3 (b). This aspect can be explained by the fact that in smooth specimens the crack nucleation mechanism changes by passing from HCF to VHCF regime, while in notched specimens there is surface or near surface crack initiation also in the

VHCF regime. However, the Authors did not provide any explanation about the reasons that causes this change of fracture mechanism and how it is correlated with the change of slope of the S-N curves.

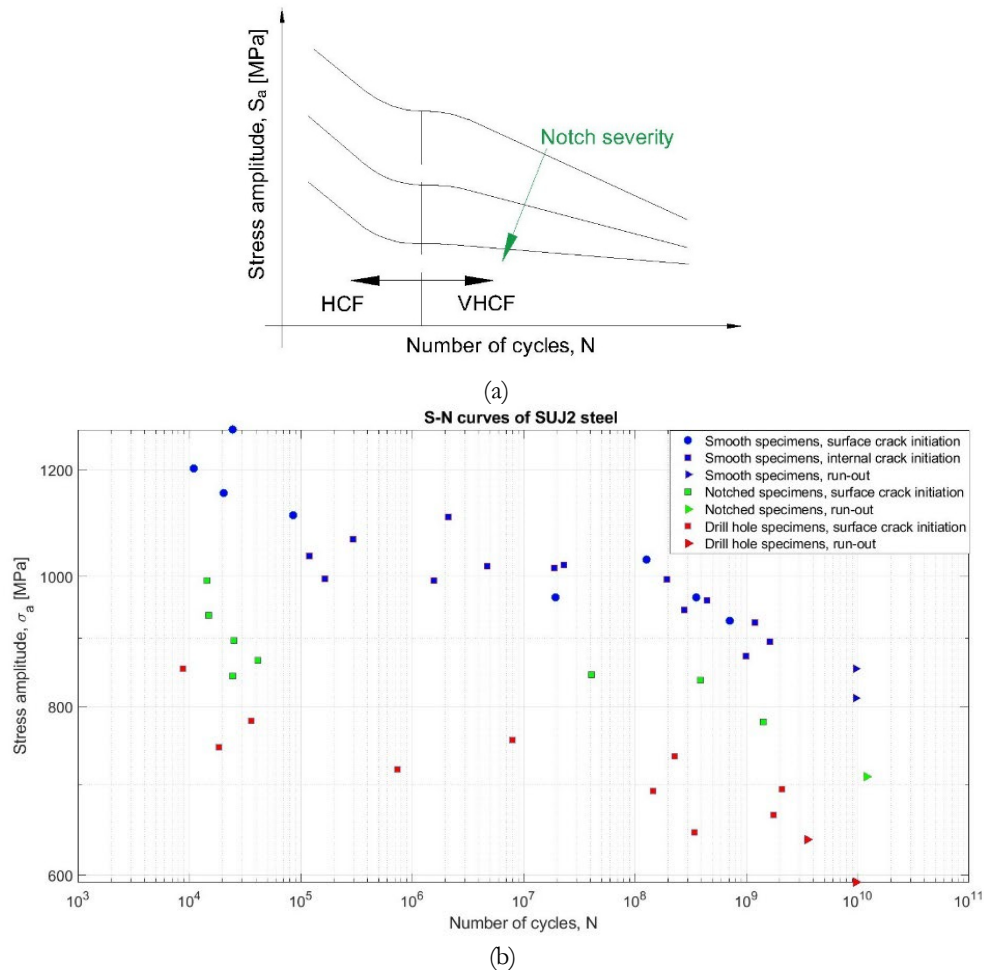


Figure 3: S-N curves of SUJ2 steel: (a) qualitative behaviour based on the results of Akiniwa[8] (b) S-N curves digitized from the data of Akiniwa et al. [8].

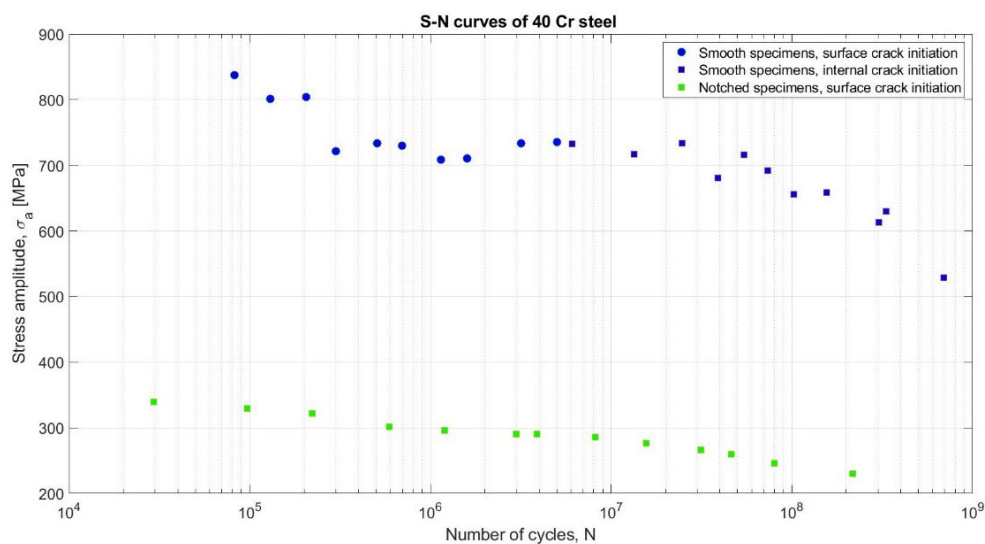


Figure 4: S-N curves of the 40 Cr steel digitized from the data of Qian et al. [10].

Qian et al. [10] studied the HCF and VHCF behaviour of a 40 Cr structural steel. The fatigue tests were performed using a rotary bending machine operating at a frequency of 52,5 Hz. All the specimens were quenched, tempered and polished at



the surface. The notched specimens have a stress concentration factor $K_t=4.04$. Three main conclusions have been drawn from the fatigue tests:

- 1) Neither the smooth nor the notched specimens show conventional fatigue limit up to 10^9 cycles.
- 2) The S-N curve of the smooth specimens has a plateau between 10^6 and 10^7 and then a change of trend in the VHCF regime, while the notched specimens have a continuous decrease from HCF to VHCF regime.
- 3) The notch fatigue factor (computed as the ratio of the fatigue strength of the smooth specimens to the fatigue strength of the notched specimens) is equal to 2.5 in the HCF regime and 2.7 in the VHCF regime and in both regions is almost constant. As a consequence, the 40 Cr steel is more affected by the notch effect in the VHCF fatigue than in HCF fatigue.

After the fatigue test, all the specimens were examined using SEM to identify the crack nucleation site. The crack of notched specimens always nucleated at the notch tip where the stresses reach their maximum value. On the other side, the crack of smooth specimens started from the surface only in the HCF regime, while for a $N_f > 3 \cdot 10^6$ cycles a typical fracture from non-metallic inclusion was observed. The different failure modes which depends on the number of cycles and geometry of the specimens is consistent with the S-N curves and with other studies on the notch effect in the VHCF regime.

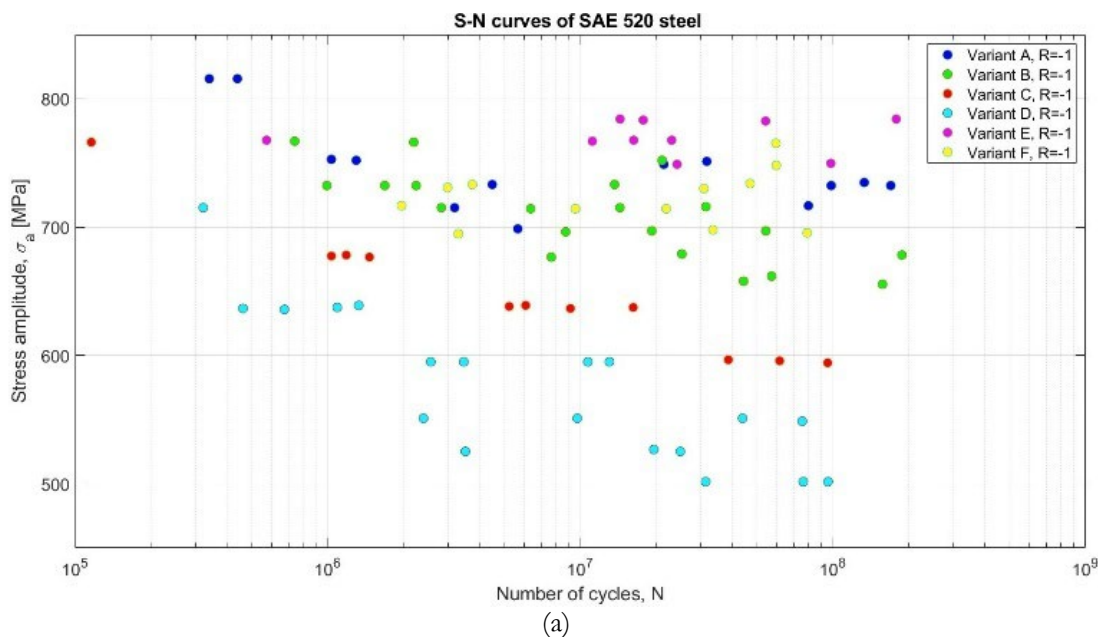
Finally the Authors also developed a model to predict the failure mode. They defined the parameter D^* , which is the ratio between the number of cycles necessary to nucleate a crack from inclusions (N_i) and the one necessary to nucleate a surface crack (N_s). This parameter is a function of the dimensions and geometry of the inclusions (ψ), the applied stresses at the surface (φ) and the material properties (k_w and $\Delta\tilde{U}$).

$$D^* = \frac{N_i}{N_s} = \frac{1.25k_w(\phi-1)^2}{\Delta\tilde{U}\psi^2} \quad (3)$$

The Authors concluded that this approach can predict well the failure mode. However, if someone needs to apply the same approach in other cases, the tuning of a lot of parameters is needed.

In the article of Burkart et. al. [14] the VHCF behaviour of notched specimens of steel SAE 5120 (EN 20MnCr5) was analysed using different notch geometries and heat treatments. The total number of different specimens that have been tested is 6 and they are reported in Tab. 1. The cleanliness indicates the number of non-metallic inclusions, which is lower in the superclean specimens than the normal specimens. The specimens with a notch radius of 6 mm have a stress concentration factor equal to 1.14, while in the other case it is equal to 1.21. Finally, the heat treatment is always a carburising, except in the “single hardening” in which the austenitizing is performed in two steps with a furnace cooling between the two steps.

All the variants of specimens were tested at $R=0$ and $R=-1$ using a frequency of 192 Hz. The first important result of this article is that none of the specimens showed a fatigue limit up to $2 \cdot 10^8$, as shown in the experimental data digitized from [14] and reported in Fig. 5.



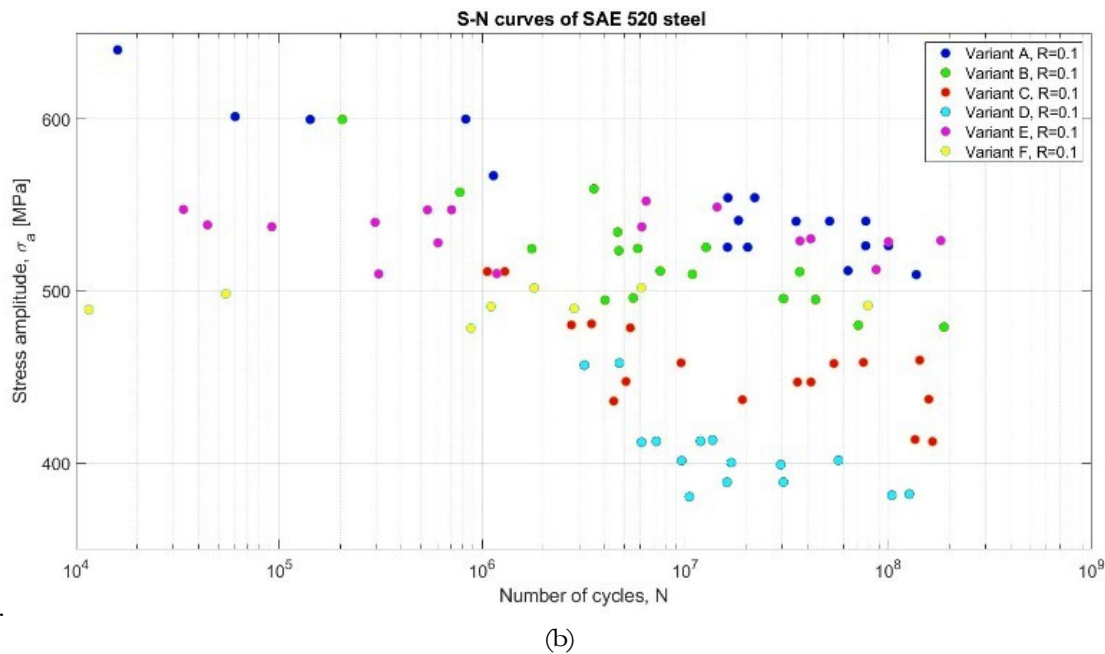


Figure 5: S-N curves of SAE 520 steel for: (a) R=-1 (b) R=0.1. Experimental data digitized from [14].

Another important result is that the specimens with a high level of cleanliness failed with a particular failure mode called “Non-Defect Crack Initiation” (NDCI). If the level of non-metallic inclusions increases (type C and D), the failure is characterised by both NDCI and classical Non-Metallic Inclusions Crack Initiation (NMICI). Finally, if the notch effect increases (type E and F), there is also Surface Crack Initiation (SCI). This results is coherent with other studies about the notch effect in the VHCF regime. The last column of Tab. 1 shows a resume of different failure modes. The Authors also tried to numerically estimate the fatigue limit using the weakest-link concept and they obtained a difference of approximately 100 MPa with the experimental results. According to the authors, further improvement in the modelling is supposed if more experimental data are available. Finally, the notch fatigue factor (i.e. K_f) has not been evaluated by the authors because they tested only notched specimens.

Variant	Cleanliness	Notch radius (mm)	Hardening	Type of failure
A	Superclean	6	Single	NDCI
B		6	Direct	NDCI
C	Normal	6	Single	NDCI+ NMII
D		6	Direct	NDCI+NMICI

Table 1: Variants of specimens used in [14] and types of failures: Non-defect Crack Initiation (NDCI), Non-Metallic Inclusions Crack Initiation (NMICI) and Surface Crack Initiation (SCFI).

Furuya et. al. [15] focused on the frequency effect on the VHCF behaviour of smooth and notched specimens. The Authors used two ultrafine-grained steels: the first with 0.29% of Carbon (defined by the authors as 30C) and the second with 0.14% of carbon (defined as 15C-P). The 30C steel was used to test notched specimens with a stress concentration factor $K_t=2$, while the 15 C-P was used to test smooth specimens. The experimental data have been digitized from [15] and reported in Fig. 6(a) (smooth specimens) and Fig. 6(b) (notched specimens). The Authors demonstrated that the frequency effect is negligible both for the smooth and the notched specimens and this result is in agreement with other studies on the frequency effect in the VHCF regime [13]. Moreover, all the notched specimens had a run-out for $N > 10^7$, while the smooth specimens failed also at 10^8 cycles. Finally, by analysing the fracture surface with the SEM, Furuya et al. showed that the notched specimens failed with a crack nucleated at the surface, while the smooth specimens fail from internal inclusion, but only for the tests conducted at 20 kHz (Fig. 7). One of the limit of this study is that the 30C steel is not a steel grade present in the standards (e.g. ISO and ASTM), and the results can be hardly compared with other studies. Moreover, the 30C was used to analyse only the behaviour of the notched specimens, so any consideration about the fatigue notch factor K_f cannot be addressed.

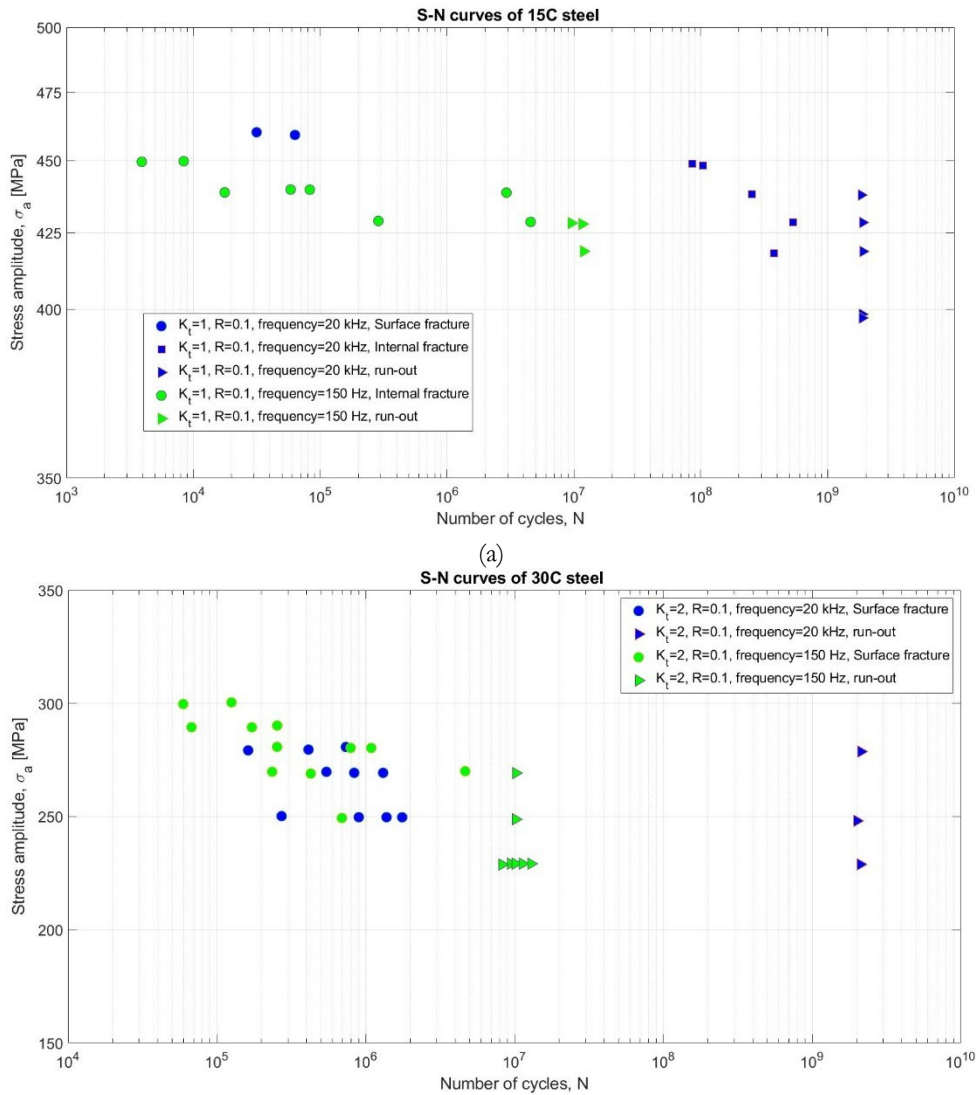


Figure 6: Experimental data digitized from Furuya et al. [15] on the S-N plot: (a) smooth specimens of 15C steel (b) Notched specimens of 30 C steel.

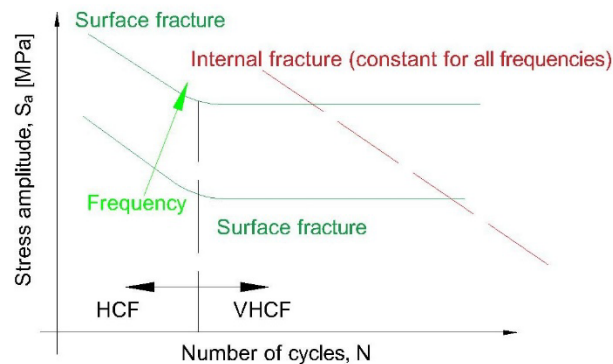


Figure 7: Correlation between fracture mechanism, number of cycles and frequency based on the results of Furuya et al. [15]

Khan et.al. [16] studied the effect of small-scale notches on the very high cycle fatigue of AISI 310 stainless steel. They used two types of specimens: smooth specimens and notched specimens with a small-scale circumferential notch on the surface. The notches were divided in two types: the first type has a stress concentration factor $K_t=4.8$ and a depth of the notch $d=180 \mu\text{m}$, while the second one has $K_t=3.2$ and $d=100 \mu\text{m}$.

All specimens were tested with an ultrasonic fatigue testing system at 20 kHz using a stress ratio $R=-1$. The experimental data have been digitized from [15] and the resulting S-N curves are reported in Fig. 8. The three types of specimens had a run-out at 10^9 cycles, that implicates, according to the Authors, a fatigue limit of 500 MPa, 300 MPa (for $K_t=3.2$) and 180 MPa (for $K_t=4.8$).

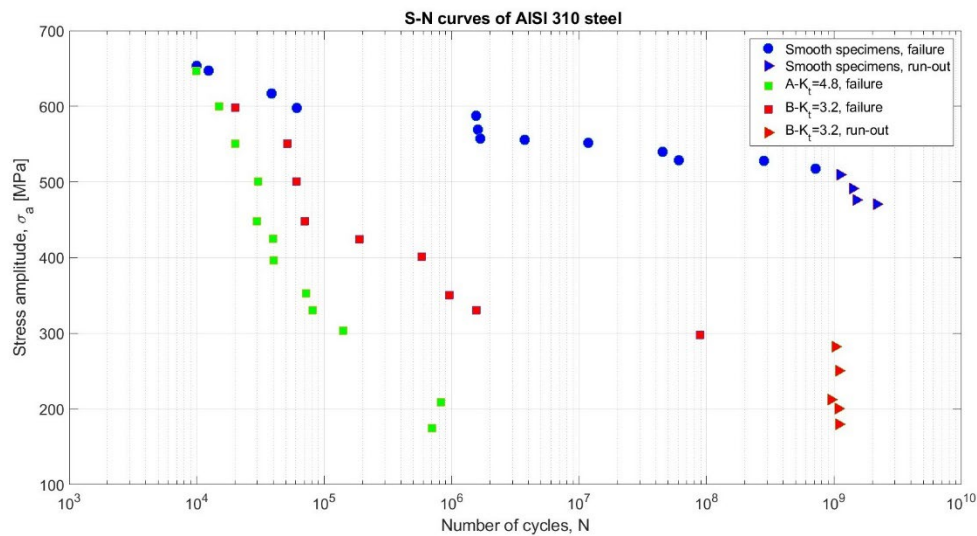


Figure 8: S-N curves in the VHCF regime of AISI 310 stainless steel. Experimental data digitized from [16].

The SEM analysis showed that both the smooth and the notched specimens had crack initiation sites at the surface, consistently with the presence of an S-N curve without a step. The notch fatigue factors K_f are reported in Tab. 2: Values of K_f and K_t at different number of cycles for AISI 310 stainless steel [16] together with the ratio K_f/K_t (computed to highlight the notch sensitivity). The values show that:

- 1) The sensitivity to the small-scale notches increases when the stress concentration factor increases.
- 2) The notch sensitivity increases with the number of cycles and it is higher in the VHCF regime than in the HCF regime
- 3) The sensitivity to small-scale notches is almost constant for $N_f > 10^6$ cycles.

N_f	$K_t = 4.8$		$K_t = 3.2$		
	K_f	K_f/K_t	K_f	N_f	K_f
1.00×10^4	1.096	22.8%	1.02×10^4	0.985	20.5%
1.44×10^5	1.979	41.2%	1.89×10^5	1.336	27.8%
1.02×10^6	3.559	74.1%	1.01×10^6	1.9	39.6%
			1.02×10^7	1.79	37.3%
			1.04×10^8	1.752	36.5%
			1.12×10^9	1.729	36.0%

Table 2: Values of K_f and K_t at different number of cycles for AISI 310 stainless steel [16].

The research of Ritz and Beck [17] aims to study the influence of mean stresses on notches on the VHCF regime of a low-pressure turbine steel with notches. The material is a martensitic stainless steel X10CrNiMoV12-2-2 and it was tested using three different notch geometries with stress concentration factors of $K_t=1.09$, $K_t=1.31$ and $K_t=2.42$. All the types of specimens were tested at 20 kHz using a stress ratio of $R=-1$, while only the slightly notched samples ($K_t=1.09$) were also tested at $R=0.5$.

Fig. 9 shows the experimental data digitized from [17]. The specimens with $K_t=1.09$ showed a flatter slope in the VHCF regime with respect to the HCF regime. Moreover, none of them showed a fatigue limit up to $2 \cdot 10^9$ cycles, corresponding to the run-out. The cracks nucleated from inclusions both for $R=-1$ and $R=0.5$ in the VHCF regime, while in the HCF regime the cracks nucleated from the surface. The specimens with $K_t=1.31$ showed a negligible slope in the S-N curve

similar to that of the $K_t=1.09$, but they all failed from cracks nucleated at the surface, both in the VHCF and HCF regimes. Finally, the specimens with $K_t=2.42$ showed a fatigue limit at 10^6 cycles and failures only from a crack nucleated at the surface. The conclusion is that for a X10CrNiMoV12-2-2 the increase of the stress concentration factor K_t causes a change of failure mechanism leading to surface crack nucleation even in VHCF fatigue, where usually a failure from inclusions is expected. Moreover, if the stress concentration factor is high enough, a fatigue limit may be present. Finally, the fatigue notch factor K_f can not be discussed because the Authors analysed only the S-N curve of specimens with a small stress concentration factor, and not the curves of perfectly smooth specimens.

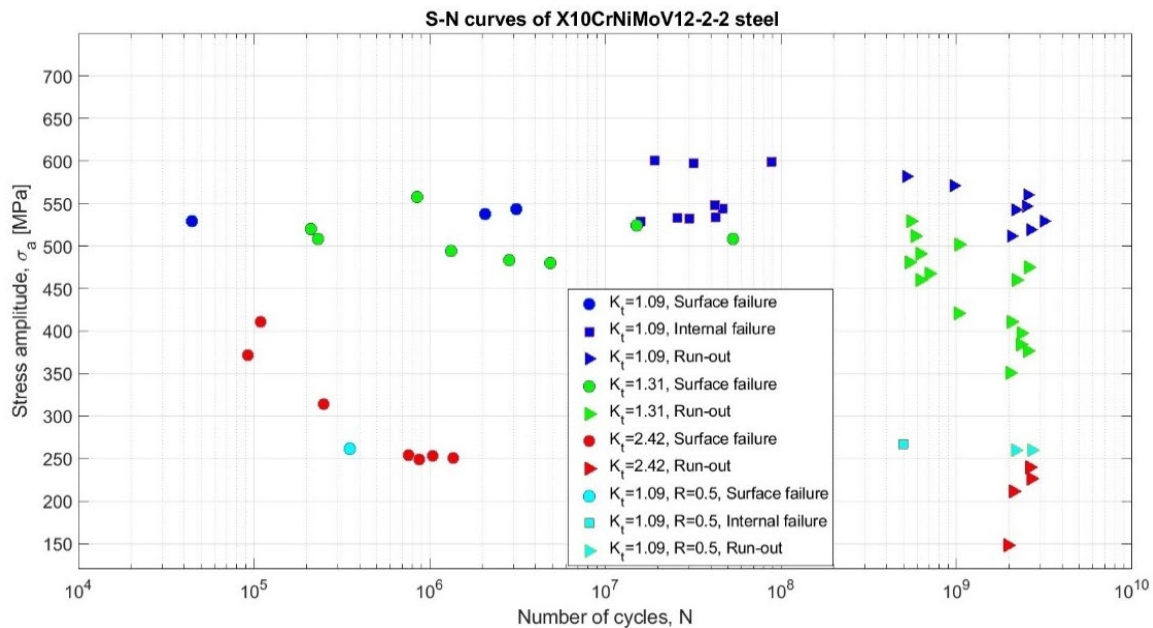


Figure 9: S-N curve of the X10CrNiMoV12-2-2 in the VHCF regime. Experimental data digitized from [17].

Dantas et. al. [4] studied the notch effect of a quenched and tempered S690QL structural steel. The fatigue tests were conducted at 20 kHz using three different geometries: one smooth specimen and two v-notch blunt geometries with different stress concentration factors ($K_t=1.15$ and $K_t=1.33$). The geometry of the notched specimens was initially computed using a new analytical approach and then optimised by numerical modelling. Moreover, all the specimens were mechanically polished to avoid the influence of the surface finishing.

In Fig. 10 the experimental results (digitized from [4]) are reported in terms of S-N curves. Both the smooth and the notched specimens showed a fatigue limit between $2 \cdot 10^7$ and $5 \cdot 10^7$ cycles. The singularity of this study is that the notch sensitivity (q) not only increases with the number of cycles, but it also exceeds 1 (Tab. 3). Some possible explanations could be the following, according to the authors:

- 1) The S690QL is highly notch sensitive due to the fine-grained microstructure.
- 2) The number of samples (14) used for notched specimens is too small compared to the number of smooth specimens (30). Additionally, the scatter is greater in the HCF fatigue than in the VHCF regime.
- 3) The authors computed the stress concentration factor as the ratio between the maximum stress and the nominal stress, but they defined the nominal stress as the average stress in the critical section. As a consequence, Dantas et. al. may have overestimated the stress concentration factor K_t with respect to other articles, in which K_t is usually computed as the ratio between the maximum and the minimum in the critical section [5].

Finally, Dantas et.[4] al. also analysed the surface fracture at SEM. All notched specimens had surface crack initiation, while the smooth specimens were characterised by one fish-eye crack initiation.

The article of Nehila et. al. [9] is focused on the study of the notch effect of a carburized 17 CrNi high-strength-steel in the very high cycle fatigue. The authors used a notched specimen with a stress concentration factor $K_t=1.89$. The specimens were carburised, quenched and low-tempered using the same parameters of their previous work of the same material for smooth specimens [18]. Finally, all specimens were polished. The fatigue tests were all conducted using a high electromagnetic fatigue testing machine with a loading frequency of 100 Hz and a stress ratio $R=-1$. The main results of this article are:

- 1) The notched specimens show a fatigue limit of about 200 MPa and there are no failures for $N_f > 10^6$ cycles, while the authors found that the smooth specimens do not show a fatigue limit up to 10^8 cycles.
- 2) The final failure of the notched specimens started from the surface and not from internal defects as in the smooth specimens. This result is in agreement with all the previous studies about the VHCF behaviour of notched specimens.

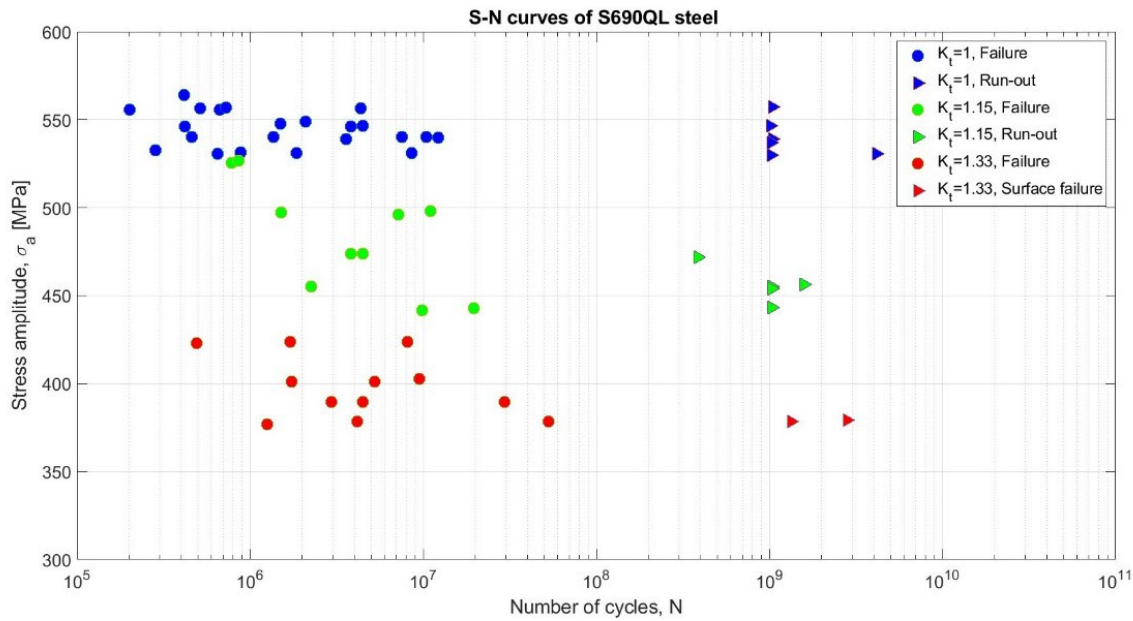


Figure 10: S-N curves of the S690QL structural steel in the VHCF regime. Experimental data digitized from [4].

Specimen	N_f	K_f	K_f/K_t	σ_D
Smooth	1.00×10^6	1	100.0%	519
	2.00×10^7			
Notched $K_t = 1.15$	1.00×10^6	1.12	97.4%	423
	2.00×10^7	1.23	107.0%	
Notched $K_t = 1.33$	1.00×10^6	1.38	103.8%	365
	2.00×10^7	1.42	106.8%	

Table 3: Variation of notch sensitivity with respect to the number of cycles for a S690QL structural steel [4].

Aluminium alloys

Schwerdt et al. [19] studied the VHCF behaviour of an EN AW 6056 aluminium alloy. They considered three different specimen geometries: smooth with $K_t=1$, slightly notched with $K_t=1.75$ and sharp notched (screw M10) with $K_t=4.7$. The stress concentration factor K_t was evaluated in the static condition because the authors did not use ultrasonic fatigue testing machine.

The smooth and slightly notched specimens were tested with a frequency of 400 Hz and a load ratio $R=0.1$, while the sharply notched specimens were tested with a frequency of 150 Hz and a load ratio of $R=0.1$. Additionally, a few smooth specimens were tested with a load ratio $R=-1$ to evaluate the influence of the mean stress. The experimental data for $R=-1$ have been digitized from [19] and the S-N curves are reported in Fig. 11 and none of the tested geometries showed a fatigue limit up to 10^9 cycles, corresponding to the run-out number of cycles. Despite the authors did not evaluate numerically the reduction introduced by the notches, it is possible to compute the notch fatigue factor as the ratio between the strength of the smooth specimens and the strength of the notched specimens. The values are $K_f=1.46$ (for $K_t=1.75$) and $K_f=6.11$ (for $K_t=4.7$) and they are constant in all the VHCF regime. The screwed specimens are highly notch sensitive, but the authors concluded that the result is coherent with the common guidelines for screws [20]

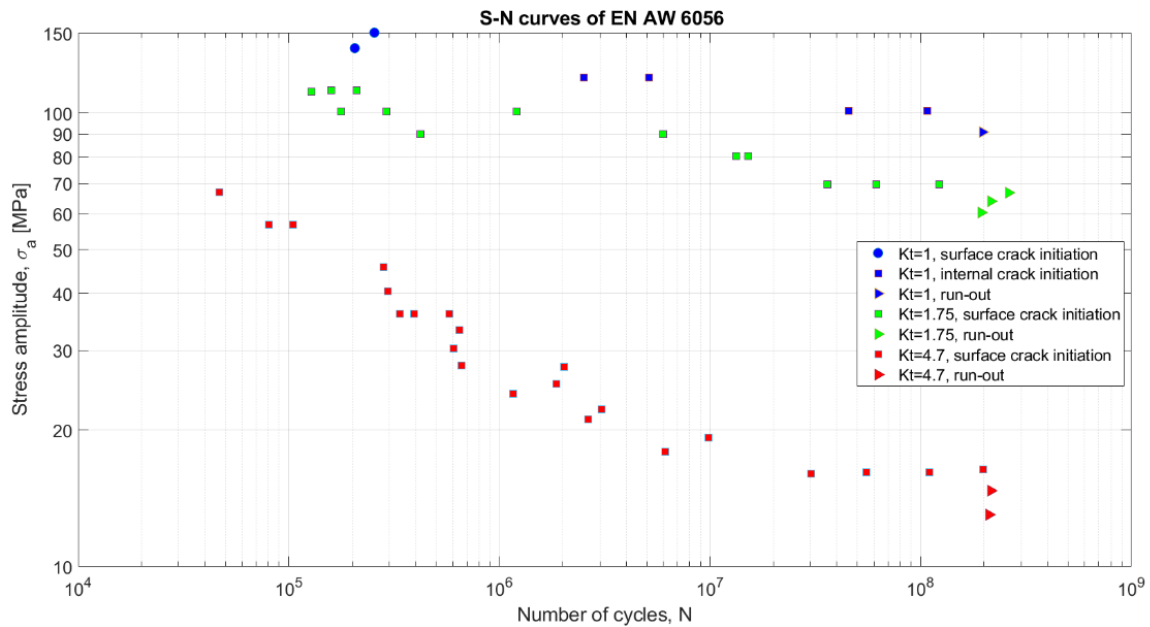


Figure 11: S-N curve of the EN AW-6056 in the VHCF regime. Experimental data digitized from [19].

Schwerdt et al. also analysed the surface fracture using SEM and they concluded that:

- 1) Smooth specimens tested with $R=0.1$ had a failure that started from the surface for N_f smaller 10^6 cycles, while for $N_f > 10^6$ cycles the fatigue crack started internally but without defects (non-defect failure).
- 2) The slightly and sharply notched specimens always failed with a fracture initiated at the surface of the notch or the thread, independently of the number of cycles.
- 3) The smooth specimens tested with $R=-1$ showed surface crack initiating also at higher number of cycles than the same specimens tested at $R=0.1$. The authors supposed that the transition of failure mechanism at lower mean stress occurs at higher number of cycles. This aspect is visible also in Fig. 12.

The article of Cremer et. al. [21] is focused on the study of the VHCF behaviour of an aluminium alloy, which is influenced by the microstructure, the geometrical notch effect and the presence of welding defects (i.e. voids, Lack Of Fusion). As a consequence, the authors also analysed the VHCF behaviour of notched samples of the same material as the welded samples. Since the main purpose of this article is a review of the notch effect in the VHCF regime, only the results of Cremer et. al. regarding the notched specimens are discussed here. The material used by the authors is an EN AW-6082 aluminium alloy. The stress concentration factor K_t was computed using the analytical Eqn. 4 (with R being the notch radius, t the notch depth, D the external diameter and d inner diameter) and it represents the static K_t .

$$K_t = 1 + \frac{1}{\sqrt{0.22 \cdot \frac{R}{t} + 2.74 \cdot \frac{R}{D} \cdot \left(1 + 2 \cdot \frac{R}{d}\right)^2}} \quad (4)$$

The notched samples were divided in three categories. Each of them was subjected to a different heat treatment to reach a different hardness condition: 75 HV (to compare the Heat Affected Zone of the welded samples), 85 HV (to compare the Fused Zone) and 110 HV (to compare the Base Material). In Tab. 4 a summary of the three categories is reported.

All the tests were performed at 20 kHz using a stress ratio $R=-1$ and the experimental results (digitized from [21]) of the fatigue test are reported in Fig. 13. The first important result is that none of the three categories shows a fatigue limit up to 10^9 cycles, which is the run-out of the test. Moreover, an increase in the hardness causes an increase in the fatigue strength. The authors suggested that this effect is caused by the microplasticity effect and its dependence on the different heat treatment conditions, but further investigations are needed.

Finally, the values of K_f (computed as) are reported in Tab. 5. For all the hardness conditions K_f decreases with the increase of the number of cycles, which means that the notch sensitivity decreases in the VHCF regime.

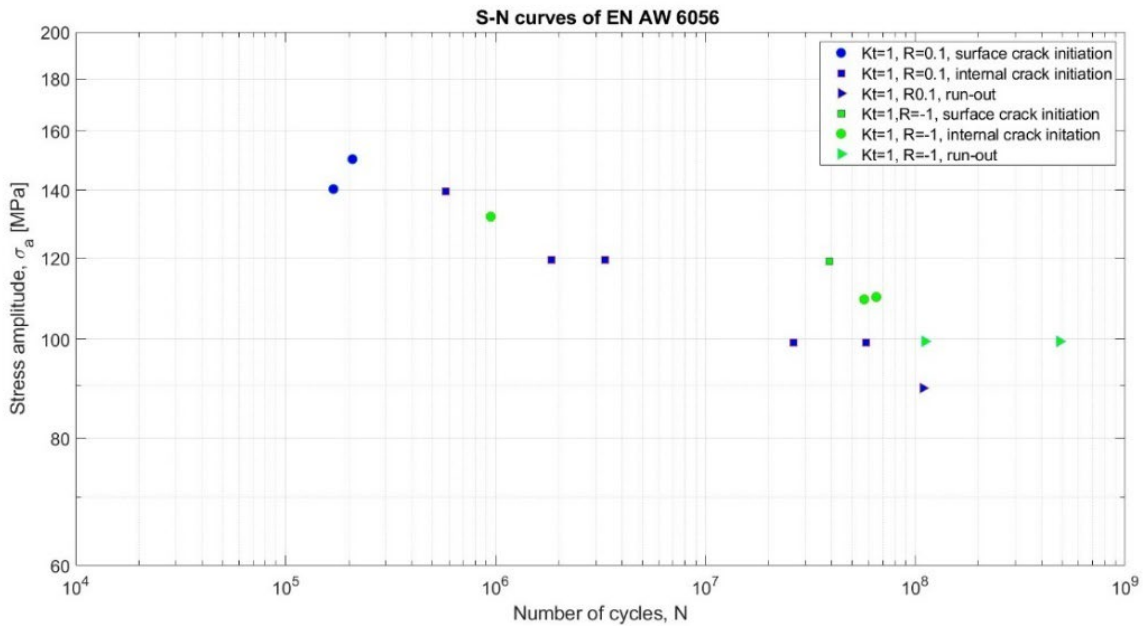


Figure 12: Influence of the stress ratio on the VHCF behaviour regime of EN AW-6056. Experimental data digitized from [19]

Material	EN AW-6082		
Hardness	85 HV	75 HV	110 HV
Annealing	540 °C/60 min	540 °C/60 min	540 °C/60 min
Ageing	200 °C/60 min	200 °C/60 min	200 °C/60 min
Overageing	360 °C/7 min	360 °C/11 min	-

Table 4: Categories of notched samples of EN AW-6082 used by Cremer et. al. [21].

The most recent work on the notch effect of aluminium alloy in the VHCF regime was conducted by Tridello et al.[6], but it focuses on Additive Manufacturing (AM) aluminium. The authors used two types of specimens of AlSi10Mg aluminium alloy produced by LB-PBF technology and subjected to an ageing heat treatment to minimise the residual stresses and their influence on the fatigue tests. The first geometry is a rectangular bar with dimensions 10x4x132 mm (plain specimens), while the second geometry is a bar with the same dimensions and a hole of 2 millimetres diameter in the centre (notched specimens). Both specimens were cut without any surface finishing after the cut. The stress concentration factor (K_t) of the notched specimens was computed according to the definition of Paolino et al. [5]. Consequently, K_t in this case is equal to the ratio between the peak stress and the stress at the inflection point of the axial stress, as shown in Fig. 14.

Load cycles	10 ⁷	10 ⁸	10 ⁹
$K_f(110HV)$	1.47	1.45	1.42
$K_f(85HV)$	1.65	1.62	1.47
$K_f(75HV)$	1.87	1.76	1.62

Table 5: Notch fatigue factors K_f for the notched samples analysed by Cremer et. al. [21]

The fatigue tests were conducted with a frequency of 20 kHz and a load ratio of $R=-1$. The runout was fixed at 10⁹ cycle and the S-N curve are reported Fig. 15. The main results of the S-N curves are the following:

1. The notch effect is evident because notched specimens fail at stresses which are significantly lower than plain specimens.

2. The fatigue notch factor (K_f), computed as the strength of the plain specimens and the strength of the notched specimens, is equal to 1.76 and it is almost constant in all the VHCF regime. According to the authors, the cause is the presence of the same failure origin (from surface defects) for both the geometries. Moreover, the authors also computed K_f according to the Neuber relations, obtaining a value of 1.87. Since the difference is smaller than 5 %, they suggested that the notch fatigue factor of AlSi10Mg AM alloys can be computed by literature equations, but experimental tests are always recommended due to the large experimental variability.

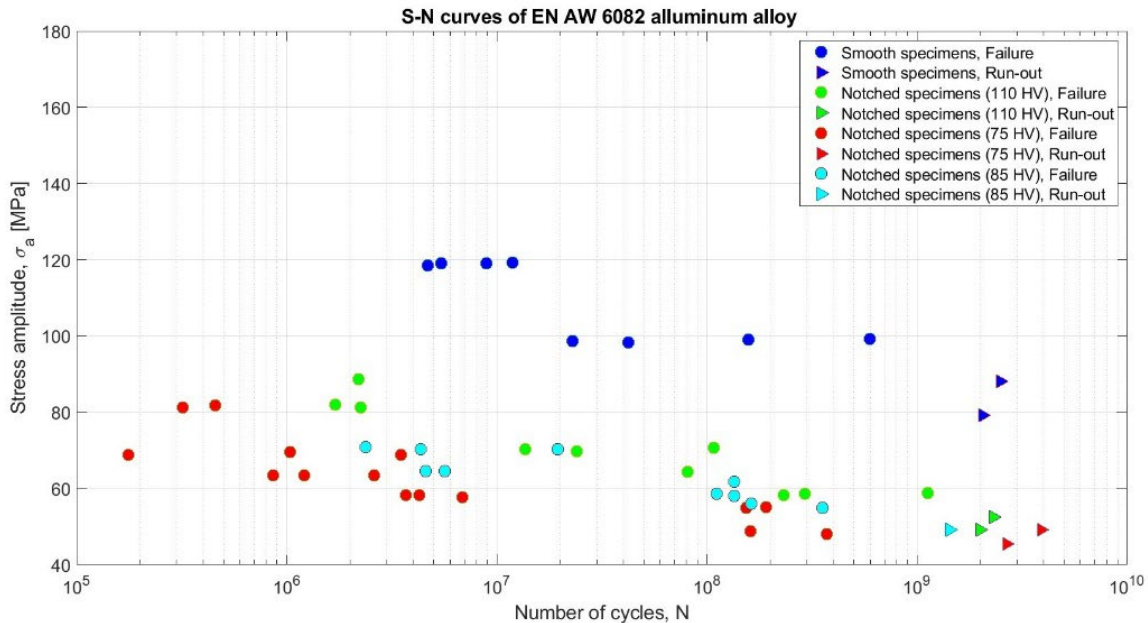


Figure 13: S-N curve of the EN AW-6082 in the VHCF regime. Experimental data digitized from [21]

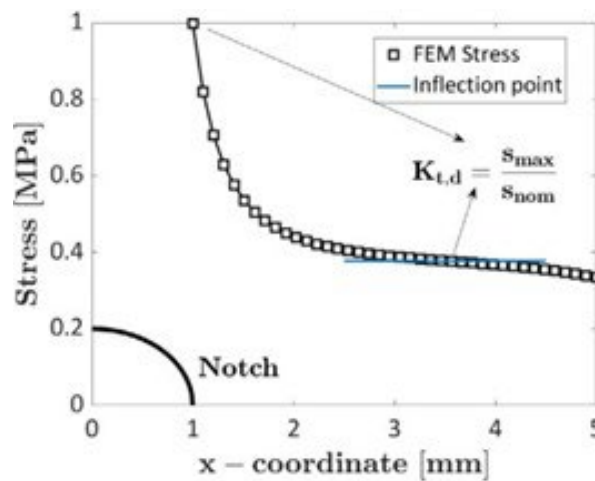


Figure 14: Definition of the stress intensity factor used in [6]

EBSDF analyses have also been carried out and showed that there is no correlation between the grain size and the location. Consequently, the authors concluded that the grain size does not have a significant role in the fatigue response, which is mainly controlled by surface defects and irregularities. Finally, analyses of the fracture surfaces with the FESEM showed that the cracks originated from the specimen surface for plain specimens and from the border of the hole for notched specimens. The Authors conclude that internal defects are not critical for the failure of this type of material because the surface irregularities have a detrimental effect, since the specimens were tested in the as-built condition, without surface finishing.

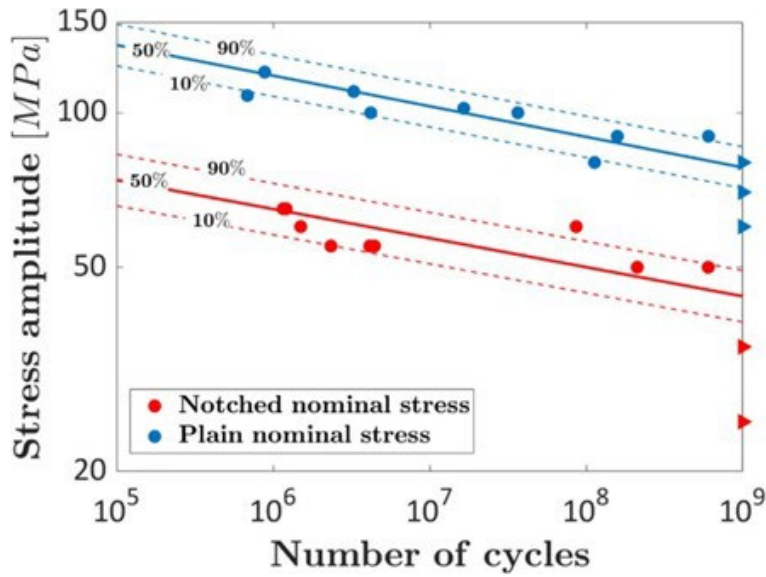


Figure 15: S-N curves in the VHCF regime of AlSi10Mg produced by LB-PBF [6].

Other metallic materials

The study of Nie et al. [22] is focused on the study of the VHCF behaviour of a TC21 titanium alloy. The authors tested 2 geometries: smooth specimens and notched specimens with a stress concentration factor $K_t=2.85$. This value was computed by analyzing the static distribution of stresses. Both specimens were subjected to a double annealing treatment and a double air quenching.

The fatigue tests were executed with a frequency of 20 kHz and a load ratio of $R=-1$. The experimental results have been digitized and are reported in Fig. 15. The curves show a fatigue limit at 10^8 cycles, which is greater than the traditional limit of the HCF regime. The notched specimens have a larger scatter and lower strength than the smooth specimens. Moreover, notched specimens have a continuous decrease in the S-N curves, while smooth specimens have a stepwise curve. The Authors also computed the notch fatigue factor K_f as the ratio between the stress amplitude of smooth specimens and the same variable of the notched specimens, for the same number of cycles. They obtained a value equal to 1.5 in the HCF regime and 1.43 in the VHCF regime. Additionally, the values are constant in both regions. According to the authors, these results are influenced by the size effect since the critical volume (region subjected to a stress higher than 90% of the maximum stress) is higher in notched specimens than in smooth specimens.

The SEM analysis showed that in the HCF regime all the specimens failed with a crack started at the surface, while for $N_f > 10^6$ the cracks nucleated in the subsurface. Particularly, the smooth specimens showed Fine Granular Area (FGA) along the α lamellar, while for notched specimens the crack initiation sites had flat facets or facet+FGA.

Nie et al. also analysed the dimensions and position of the crack initiation sites, showing that there is correlation between the depth of the nucleation sites and the number of cycles only for notched specimens, but not for smooth specimens. Finally, they also computed the equivalent stress using the formulation proposed by Chapetti [23] and reported in Eqn. 5, being K_t the static stress concentration factor, $\Delta\sigma_n$ the nominal stress range, a the distance of the defect from the notch root surface, ρ the radius of the notch root and d the subsurface crack initiation size.

$$\Delta\sigma = \frac{K_t \Delta\sigma_n}{\sqrt{1 + \frac{4.5(a+d)}{\rho}}} \tag{5}$$

Fig. 17 shows the correlation between the equivalent stress and the number of cycles. The Authors concluded that there is a good correlation only in the VHCF regime, in which there is subsurface failure both for smooth and notched specimens. Yang et al. [24] investigated the notch fatigue behaviour of a near- α titanium alloy (Ti-8Al-1Mo-1V). The Authors used notched axisymmetric specimens, but they did not compute any value of K_t to quantify the stress concentration factor. However, Gao et al. [11] reanalysed the data of this Ti-8Al-1Mo-1V titanium alloy to compare with the TC 17 and they obtained a value of $K_t=3$.

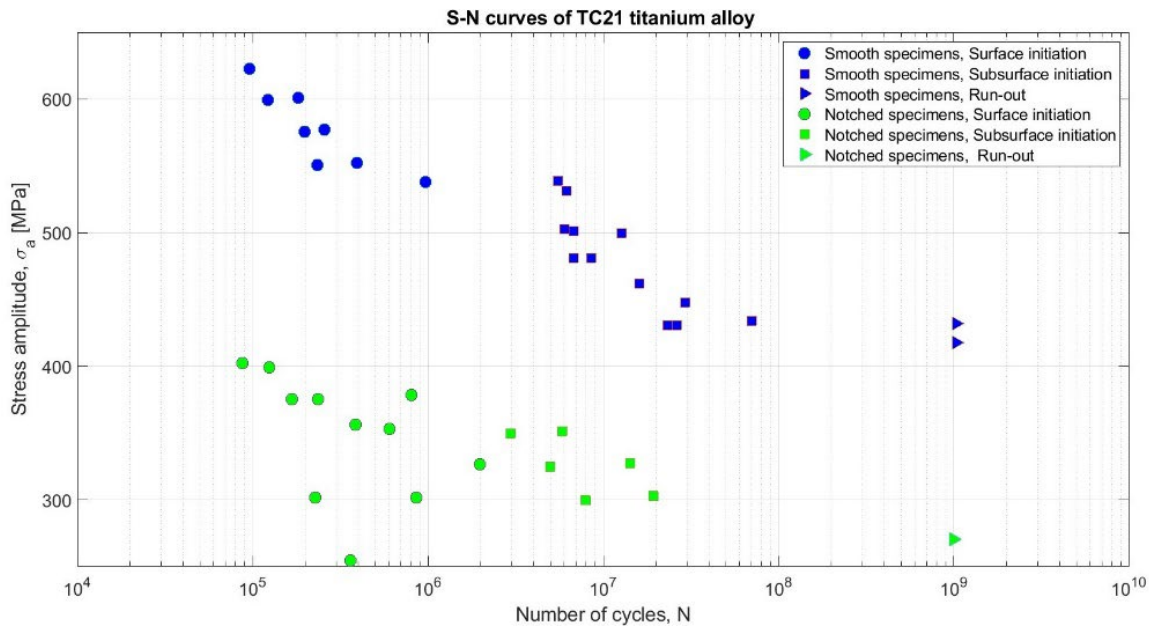


Figure 16: S-N curves in the VHCF regime of TC21 titanium alloy. Experimental data digitized from [22]

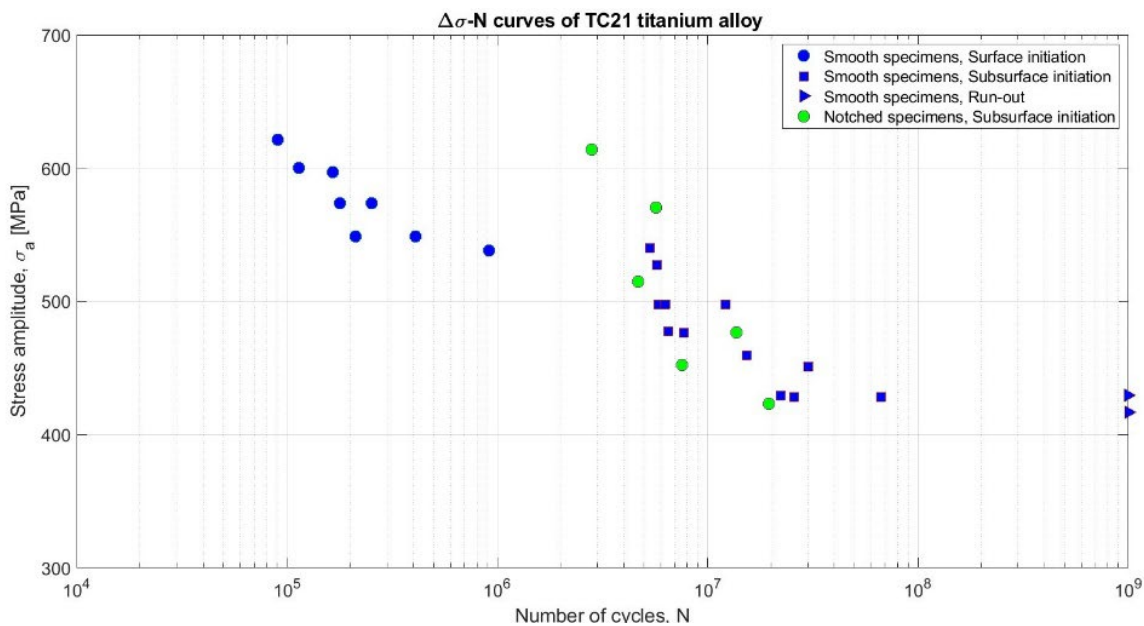


Figure 17: S-N curves in the VHCF regime of TC21 titanium alloy for equivalent stress. Experimental data digitized from [22]

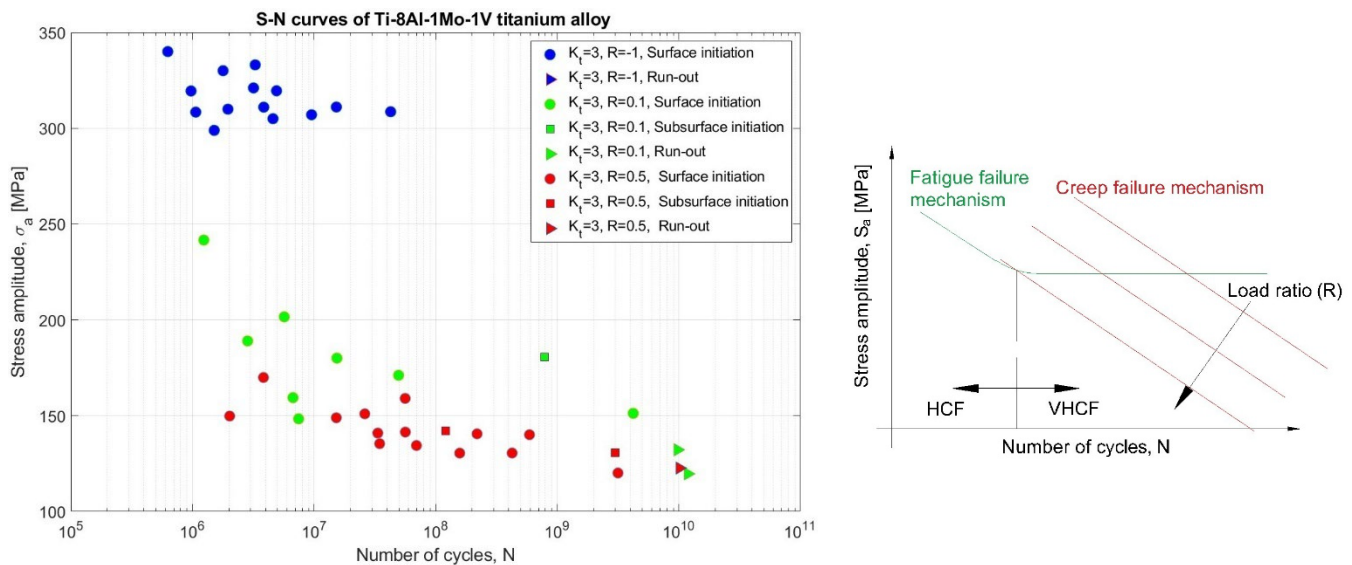
(a) The fatigue tests were conducted at frequency of 20 kHz and three different stress ratios: $R=-1$, $R=0.1$ and $R=0.5$.

The experimental data of [24] have been digitized and S-N curves are reported in

Fig. 18(a) and present three completely different behaviours depending on the stress ratio. For $R=-1$ a fatigue limit is present at 10^7 cycles, corresponding to a stress of 279 MPa. For $R=0.1$, S-N curve presents the typical step-wise curve of the VHCF regime. Finally, for $R=0.5$ there is a continuous decrease among all fatigue life up to 10^{10} cycles. For smooth specimens, the different trends in the VHCF regime were attributed to the competition between the surface and interior fatigue failure life [25–27]. According to the Authors, the reason should be different in this case because interior crack initiation was not detected in notched specimens. Indeed, Yang et al. found two types of failure modes by using SEM and EDS:

1. Surface crack initiation with a single initiation point for all the specimens tested at $R=-1$;
2. Subsurface crack initiation from interior inclusions for some of the specimens tested at $R=0.1$ and $R=0.5$.

(b) Yang et al. concluded that the different S-N curves are caused by a competition between the fatigue failure mechanism and the creep mechanism. Indeed, they assumed that for $R=-1$ only fatigue is present, while for $R=1$ only the creep affects the failure. Consequently, for increasing values of R there is an increasing influence of the creep, as shown in Fig. 18(b).



(a) Figure 18: Experimental results of Ti-8Al-1Mo-1V titanium alloy in the VHCF regime: (a) Experimental data digitized from [24] on the S-N plot (b) Influence of the stress ratio (R) based on the results of [24].

Finally, it is important to mention that although Yang et al. did not compute a value for the notch fatigue factor (i.e. K_f), Gao et al. [11] reanalysed this article and they computed a notch fatigue factor $K_f=2$ at 10^7 (Fig. 20). This value is computed as the ratio of the fatigue strength of notched specimens with $R=-1$ and the fatigue strength at the same number of cycles computed by Yang et al for smooth specimens [28]. The value of K_f is not constant with the number of cycles, but it decreases when N increases.

The paper published by Shen et al. [29] is the only study on the notch effect of a nickel-based superalloy. Despite the main goal of the article being the discussion of the Theory of Critical Distance (TCD) applied in the HCF and VHCF regime, some important data about the notch effect in VHCF are reported. The Authors tested three types of specimens made of INCONEL 718 in the VHCF regime to develop a new approach to the TCD that works well both in the HCF and VHCF regime. Particularly, the geometries adopted by Shen et al. are: a smooth specimen, a notched specimen with $K=2.36$ and a notched specimen with $K_t=3.84$. In both cases, the stress concentration factor is considered as the ratio between the maximum stress and the nominal stress in the gross section in static condition, without considering the stress distribution in the ultrasonic fatigue testing.

All the tests were performed with a frequency of 20 kHz and a stress ratio $R=0.1$ or $R=0.5$. Fig. 19 shows the experimental data digitized from [29]. All the three types of specimens did not show a fatigue limit up to 10^9 cycles, independently on the stress ratio. Although the authors did not compute the reduction in terms of ratio between the strength of the smooth specimens and the strength of the notched specimens, it is possible to say that the INCONEL 718 is high notch sensitive. The sensitivity is constant for $R=0.1$, while for $R=0.5$ it slightly increases with the number of cycles when $K_t=3.84$.

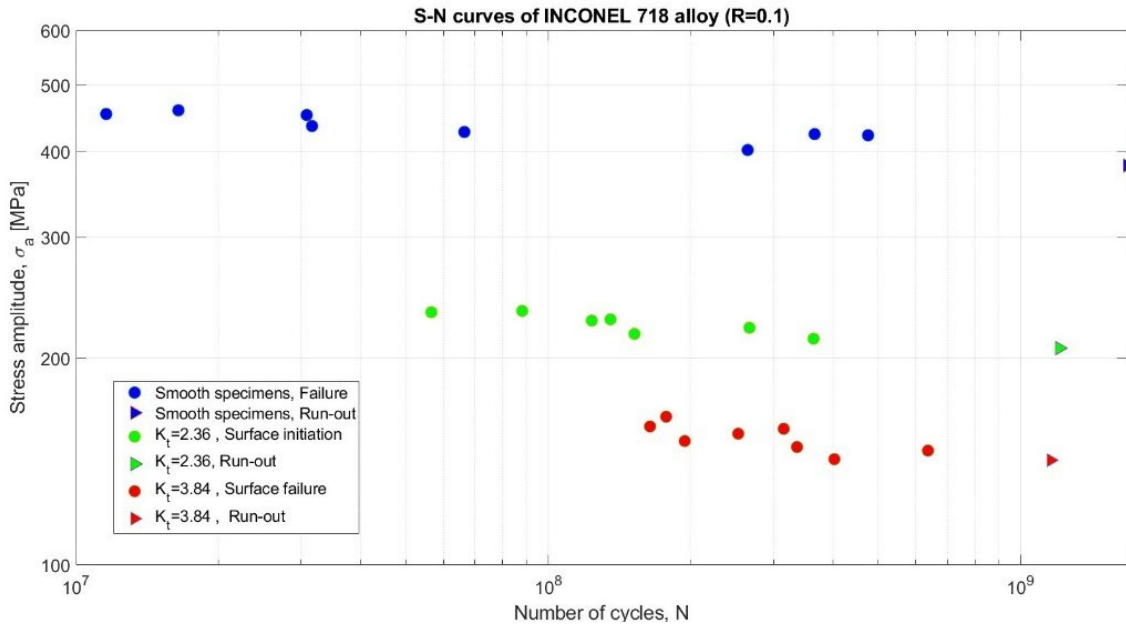
Regarding the estimation of the number of cycles to failure proposed by the authors, a detailed description will be provided in the discussion Section of the present paper. In any case, it is important to mention that the authors obtained life estimates within ± 3 life factors, which are values comparable to the values obtained in the HCF regime.

Gao et al.[11] studied the notch effect of an α - β type titanium alloy TC17. They compared the VHCF up to 10^9 cycles of smooth and notched specimens with $K_t=3$. The stress concentration factor was computed as the ratio between the maximum stress and the nominal stress in the gross section, according to the static distribution of stresses.

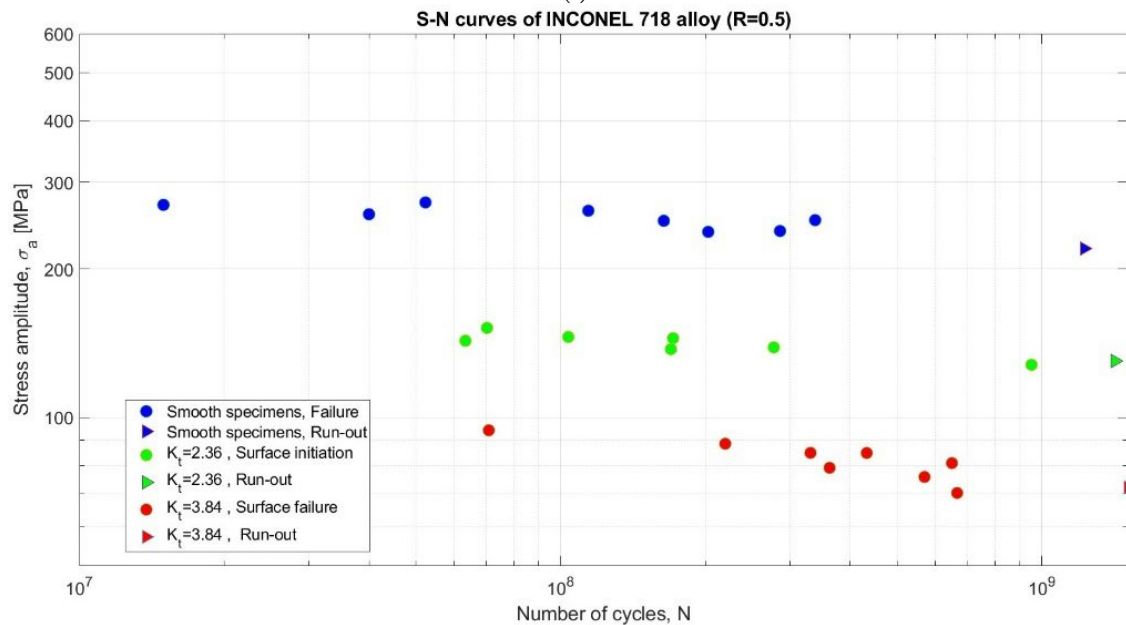
The Authors used an ultra-high frequency vibration test system based on an electrodynamic shaker. The system applies a bending cyclic load and, according to the authors, this is an advantage because it allows to have a loading condition similar to the actual service environment of aeroengine blades, which is the main application of this type of material. The frequency used in the test is equal to 1725 Hz and the load ratio is equal to $R=-1$. Fig. 21 shows the experimental data digitized from



[11] and it is possible to see that the smooth specimens as well as the notched specimens do not show a fatigue limit up to 10^9 cycles. Moreover, the slope of the notched specimens is smaller than the slope of the smooth specimens. To evaluate this effect, the Authors computed the fatigue strength reduction factor (K_f) as the ratio of the fatigue strength of smooth specimens to the ratio of the notched fatigue strength. Its correlation with the number of cycles is reported in Fig. 20(a), where it is also compared with the same variable computed with the data of Yang et al. [24]. The plot shows that, although K_f is not constant in the VHCF regime, the value provided by Neuber [30] is closer to the real values than the values provided by Peterson's formulation [31]. Gao et al. also did the same comparison for the notch sensitivity factor (q) computed with Eqn. 2.



(a)



(b)

Figure 19: S-N curves for INCONEL 718 in VHCF regime: (a) load ratio $R=0.1$ (b) load ratio $R=0.5$. Experimental data digitized from [29].

Also q has a clear dependency to N , as shown in Fig. 20 (b).

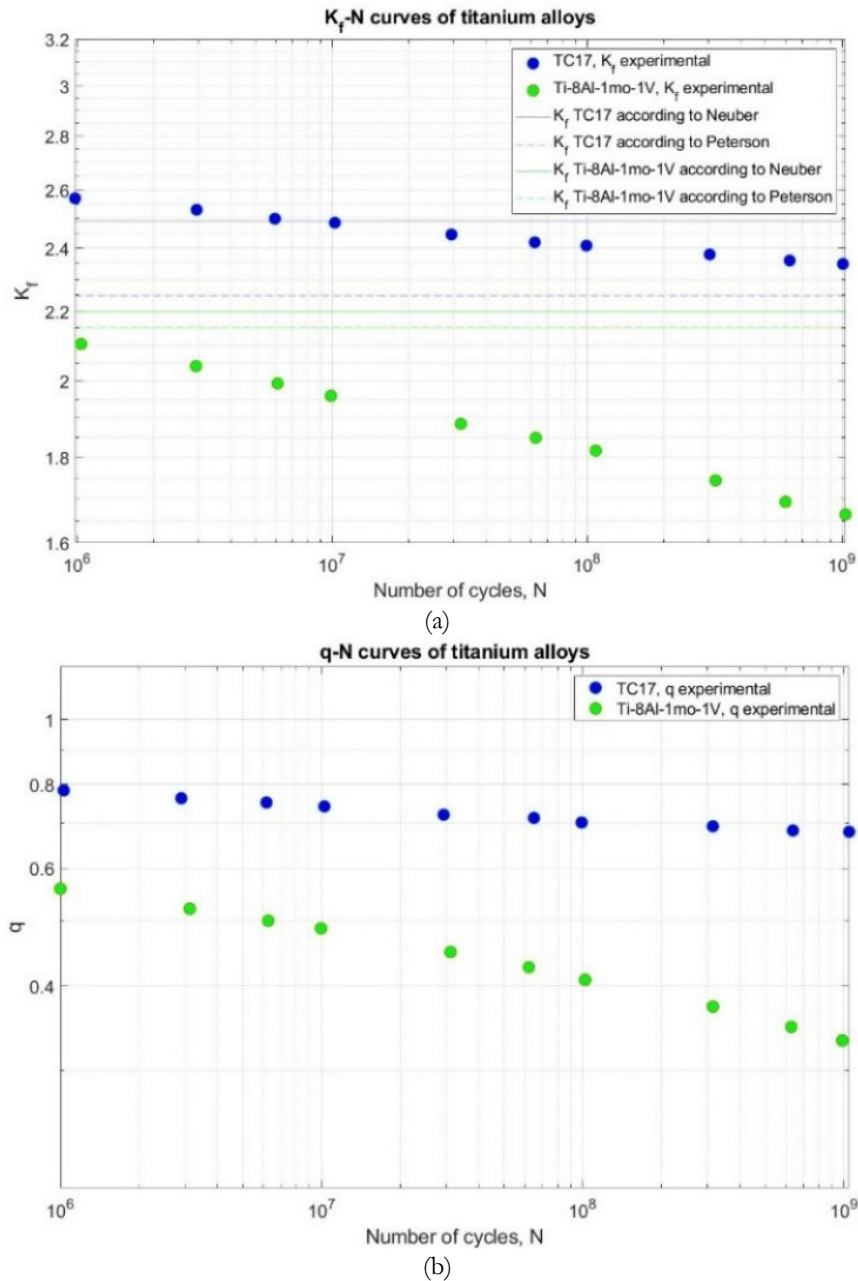


Figure 20: Correlation between the number of cycles to failure (N) and: (a) the notch fatigue factor (K_f) and (b) the notch sensitivity (q). Experimental data digitized from [11].

The SEM analysis of the fracture surfaces showed that the cracks nucleated from the surface not only for the notched specimens, but also the majority of the smooth specimens had cracks nucleated from the surface. Consequently, it is not possible to attribute the change of slope of the S-N curves to a change of failure mechanism between notched and smooth specimens, as it may happen for other materials.

Finally, Gao et al. also defined a weighting function to modify the classical TCD in order to predict the number of cycles to failure of notched specimens in the VHCF fatigue. The method will be discussed in detail in the section of discussion of the present paper, but it is important to say that they obtained a limited scatter within $\pm 5\%$.

The first study about the notch sensitivity of Additive Manufacturing (AM) materials in the VHCF regime was performed by Tridello et al. [7]. They studied the fatigue response up to 10^9 cycles of unnotched and notched specimens made of titanium alloy Ti6Al4V ELI using selective laser melting process (SLM). The stress concentration factors were computed by the Authors according to the definition of Paolino et al. [5] and they are always greater than the static K_t values. Moreover, they defined the stress concentration factor with the symbol ($K_{t,d}$) to specify that it refers to the stress concentration during a dynamic test at ultrasonic frequency. The unnotched hourglass specimens have a $K_{t,d}=1.024$, while the notched hourglass

specimens have a $K_{t,d}=1.43$. All the specimens were subjected to a stress relief heat treatment to minimise residual stresses and manual polishing to avoid the influence of macro surface scratches on the fatigue response.

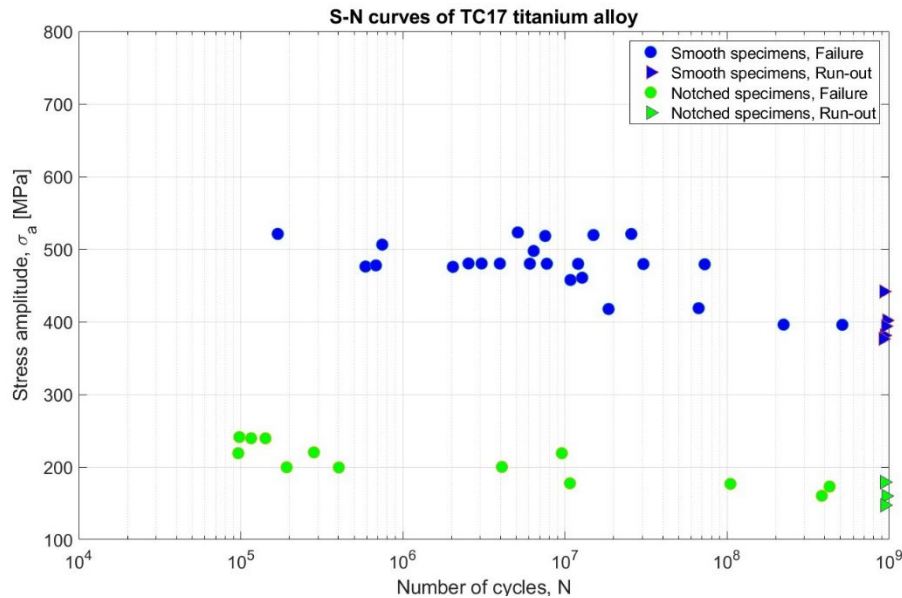


Figure 21: S-N curve of the TC17 titanium alloy in the VHCF. Experimental data digitized from [11].

The fatigue tests were conducted with a frequency of 20 kHz and with a load ratio $R=-1$. The results are reported in Fig. 22: S-N curve of the Ti6Al4V SLM in the VHCF regime obtained by Tridello et al. [7] and it is possible to see that the notch sensitivity is very small. Particularly, there is no difference for number of cycles above 10^7 , but a precise comparison is not easy due to the large scatter of experimental data. According to the Authors, the large scatter is explained by considering that failures are driven by defects randomly distributed within the loaded volume. Moreover, both the notched and unnotched specimens did not show a fatigue limit up to 10^9 cycles, corresponding to the run-out number of cycles.

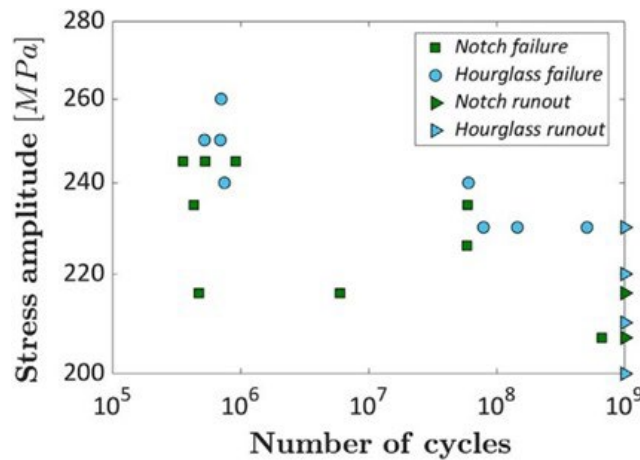


Figure 22: S-N curve of the Ti6Al4V SLM in the VHCF regime obtained by Tridello et al. [7].

The SEM analysis of the fracture surfaces showed that all the fatigue failures originated from manufacturing defects, but the fish-eye morphology typical of the VHCF regime is present only in specimens which failed above the $5 \cdot 10^7$ cycles. Tridello et al. [7,32] also analysed the size and the position of the critical defects, which are the defects originating the fatigue failure. It has been found that the critical defects were all concentrated near the surface and they suggested that the reason is the absence of further post-treatments after manual polishing (i.e. machining). Moreover, the dimensions of the critical defects of hourglass specimens were larger than the defects in notched specimens. The Authors suggested that the reason is the different risk volume (V_{90}), defined according to Murakami [32] as the volume subjected to a stress amplitude above 90 % of the maximum amplitude stress. Indeed, the critical volume of the unnotched specimens is 20 times larger than the



one of the notched specimens. The authors concluded that for this type of AM material the stress concentration factor plays a limited influence, because the fatigue strength depends mainly from defects size and their relation with the risk volume (V90).

Material	Frequency of test [Hz]	Stress concentration factor		Notch fatigue factor		Presence of fatigue limit		Crack initiation	
		Definition according to	K _t	K _f at 10 ⁷ cycles	Trend in VHCF	U.S.	N.S	U.S	N.S
SUJ2 [8]	20000	Static	2.39	1.23	Decrease	No	No	Inclusions	Surface
40 Cr [9]	52.5	Static	4.04	2.8	Constant	No	No	Inclusions	Surface
20 MnCr5 [14]	192	Static	1.14	-	-	-	No	-	Various
20 MnCr5 [14]	192	Static	1.21	-	-	-	No	-	Various
30C [15]	20000	Static	2	-	-	-	No	-	Surface
AISI 310 [16]	20000	Static	4.8	-	-	Yes	Yes	Surface	Surface
AISI 310 [16]	20000	Static	3.2	1.7	Constant	Yes	Yes	Surface	Surface
X10CrNiMoV12-2-2 [17]	20000	Static	1.09	-	-	-	No	-	Inclusions
X10CrNiMoV12-2-2 [17]	20000	Static	1.31	-	-	-	No	-	Surface
X10CrNiMoV12-2-2 [17]	20000	Static	2.42	-	-	-	Yes	-	Surface
S690QL [4]	20000	Dantas et al. [4]	1.15	1.23	Increase	Yes	Yes	Various	Surface
S690QL [4]	20000	Dantas et al. [4]	1.33	1.42	Increase	Yes	Yes	Various	Surface
17 Cr2Ni2Mo [9]	100	Static	1.89	-	-	No	Yes	Inclusions	Surface
EN AW 6056 [19]	150	Static	1.75	1.46	Constant	No	No	Internal	Surface
EN AW 6056 [19]	150	Static	4.7	6.25	Constant	No	No	Internal	Surface
EN AW 6082 (HV 110) [21]	20000	Static	1.8	1.47	Decrease	No	No	-	-
EN AW 6082 (HV 85) [21]	20000	Static	1.8	1.65	Decrease	No	No	-	-
EN AW 6082 (HV 75) [21]	20000	Static	1.8	1.87	Decrease	No	No	-	-
AlSi10Mg LB-PBF [6]	20000	Paolino et al. [5]	2.65	1.76	Constant	No	No	Surface	Surface
TC21 [22]	20000	Static	2.85	1.43	Constant	Yes	Yes	Inclusions	Inclusions
Ti-8Al-1Mo-1V [24]	20000	Static	3	2	Decrease	No	No	Surface/ subsurface	Surface/ subsurface
INCONEL 718 (R=0.1) [29]	20000	Static	2.36	-	Constant	No	No	-	-
INCONEL 718 (R=0.1) [29]	20000	Static	3.84	-	Constant	No	No	-	-
INCONEL 718 (R=0.5) [29]	20000	Static	2.36	-	Constant	No	No	-	-
INCONEL 718 (R=0.5) [29]	20000	Static	3.84	-	Constant	No	No	-	-
TC17 [11]	1700	Static	3	2.5	Decrease	No	No	Various	Surface
Ti6Al4V SLM [7]	20000	Paolino et al. [5]	1.428	-	-	No	No	Defects	Defects

Table 6: Final comparison of notch effect in VHCF fatigue: U.S. means Unnotched Specimens, while N.S. means Notches Specimens.



DISCUSSION

In this section, the results of different authors are compared, outlining the main trends and discussing the results available in the literature. The main aspects that will be analysed are: the stress concentration, the notch sensitivity, the failure mechanism and the possible approach to design of components in presence of notches and prone to failures in the VHCF life region. For improved comprehension, the results are concisely presented in Tab. 6. If not specified in the material column, the stress ratio is assumed to be $R = -1$. The fatigue strength reduction factor, K_f , is defined as the ratio between the fatigue strength of smooth specimens and that of notched specimens, unless otherwise stated in the article. The trend of K_f is reported to assess whether the S-N curves of smooth and notched specimens exhibit the same slope.

Stress concentration factors in VHCF test

The main issue of computing the stress concentration factor in VHCF tests is the different stress distribution when the tests are conducted at ultrasonic frequency. Indeed, if the tests are carried out at low frequency (below 100 Hz) the stress distribution is the same of a static test. On the other side, when the loading frequency is very high, the stress distribution is governed by the wave propagation theory and the stress distribution is different, in particular near the notch. As a consequence, the approaches to assess the notch severity used by different authors are summarised here, discussing the advantages and the drawbacks of each method.

The majority of the authors compute the stress concentration factor as the ratio between the maximum axial stress at the notch and the nominal stress in the gross section when a static load is applied, as reported in Eqn. 6. The Authors that use this approach are reported in the second column of the Tab. 6 using the name "static approach".

$$K_t = \frac{S_{max}}{S_{nom}} \quad (6)$$

The main advantages of this approach are:

- 1) It is simple to apply since the K_t can be computed using a numerical approach (Finite Element Analysis) or the analytical formulas present in the literature, for example the Peterson's stress concentration factors [6,7]
- 2) The value of K_t does not depend on the loading frequency, but only from the geometry of the specimens.

The main drawback of this approach is that it represents the real stress distribution only if the loading frequency is low, while in the ultrasonic fatigue test there is not a direct correlation between the value of K_t and the stress distribution around the notch.

Tridello et al. [6] [7] used a different approach which takes into account the real stress distribution around the notch during the ultrasonic fatigue testing. The first definition of this approach is proposed by Paolino et al. [5] for axisymmetric specimens, in which the stress concentration factor K_t is computed as the ratio between the maximum stress amplitude (S_{max}) and the maximum stress in the specimen longitudinal axis ($S_{long,max}$).

$$K_t = \frac{S_{max}}{S_{long,max}} \quad (7)$$

In [6] they also extend the definition to plane specimens. In this case K_t is computed as the ratio between the maximum stress (S_{max}) and the stress at the inflection point of the stress in the critical section (S_{nom}), see Fig. 14.

The advantage of this approach is that the K_t is related the real stress distribution during the ultrasonic test. On the other hand, the problem is that the K_t value does not depend only on the geometry of the specimen, but also on the loading frequency. Consequently, the value of K_t may be different for similar geometries tested at different loading frequencies, and the results of the tests should be compared properly. However, in [6] the Authors also compared the value of K_t computed with their approach and the value computed with the static approach and they demonstrated that the difference is smaller than 5 % in their case.

Finally, the third possible approach has been proposed by Dantas et al. [4]. They also defined K_t as the ratio between the maximum stress amplitude and the nominal stress amplitude. However, they computed S_{nom} as the average of the stress field in the critical section. In case of an axisymmetric geometry the equation to compute this value is the following, being D_2 the diameter of the critical section and $\sigma(r)$ the axial stress as a function of the radius (r).

$$\sigma_{nom} = \frac{1}{\left(\frac{D_2}{2}\right)^2} \int_0^{\frac{D_2}{2}} \sigma(r) 2\pi r dr \tag{8}$$

As in the approach of Tridello et al., the real stress distribution during ultrasonic fatigue testing is taken into consideration in this case. Additionally, the value of K_t depends on the resonance condition, but no correlation with the static value has been found. If the same specimen's geometry is considered, the value of K_t computed with the Dantas approach is expected to be lower than the value computed with the Tridello approach, since the average stress in the critical section is larger than the maximum stress along the longitudinal axis, i.e., the nominal stress in Tridello et al. [6,7]. As a consequence, the notch sensitivity computed with the two approaches is not the same. Indeed, the specimen geometry providing the same K_t may be different, thus with different experimental results.

To conclude, all approaches are valid, when experimental tests are carried out with the ultrasonic fatigue testing machine, but there may be some issues in comparing the results of the notch sensitivity of different authors.

Design of notched specimens for ultrasonic fatigue testing

When VHCF tests are carried out, a crucial step is the design of the specimen. Indeed, if an ultrasonic fatigue testing machine is used, the specimens need to be designed to have an axial resonant frequency at 20 ± 5 kHz.

To increase the stress in the middle section during the vibration, various analytical approaches have been developed to design smooth specimens. According to these approaches, smooth specimens in ultrasonic fatigue testing could have an hourglass geometry [33] or a Gaussian geometry [5][34]. However, these analytical methods are not applicable to the design of notched specimens. As a consequence, the design of notched specimens for ultrasonic fatigue testing is mainly based on a Finite Element Analysis (FEA). In this case, the length of the specimen is iteratively changed to guarantee an axial resonant frequency at 20 kHz. Some examples of specimens used in literature are the flat specimen of Fig. 23(a) and the axisymmetric specimens of Fig. 23(b).

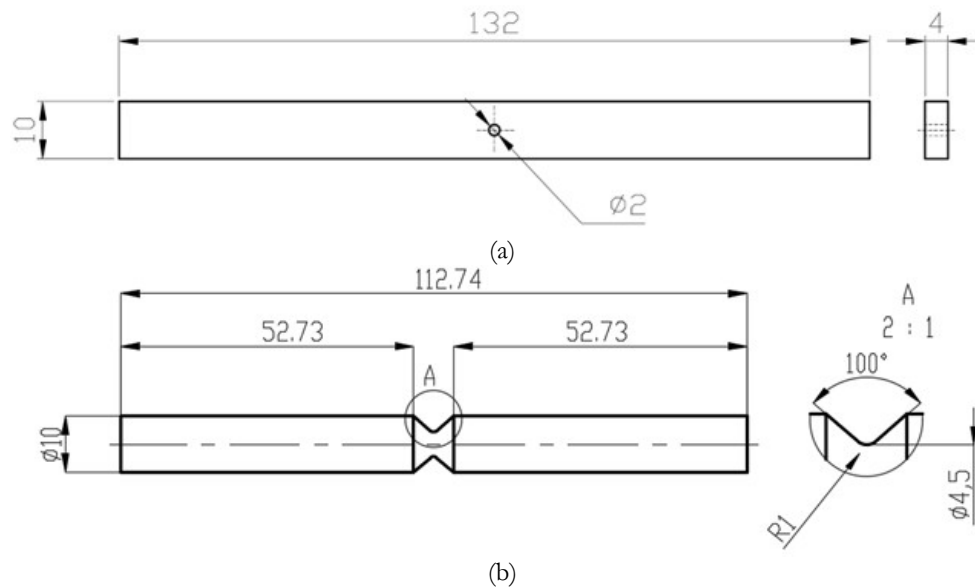


Figure 23: Example of notched specimens for ultrasonic fatigue testing: (a) plane notched specimen of Tridello et al. [6] (b) axisymmetric notched specimen of Yang et al. [24].

The only analytical approach for the design of notched specimens has been proposed by Dantas et al. [4]. The geometry defined by the authors is reported in Fig. 24 and the procedure is based on the elastic wave theory simplified for one-dimensional problems reported in Eqn. 9,

$$\frac{\partial^2 u(x,t)}{\partial t^2} = \iota^2 \left(p(x) \frac{\partial u(x,t)}{\partial x} + \frac{\partial^2 u(x,t)}{\partial x^2} \right) \tag{9}$$



being c the velocity of wave propagation ($c = \sqrt{\frac{E}{\rho}}$) and $p(x)$ the ratio of the derivate of the section ($S'(x)$) to the section ($S(x)$).

Defining k as the ratio of the frequency of vibration (ω) to the velocity c and $u(x, t) = U(X)\sin(\omega t)$, the following equation is obtained:

$$U''(x) + p(x)U'(x) + k^2U(x) = 0 \tag{10}$$

To solve the equation, the authors defined three different functions to describe the section:

$$y(x) = \frac{D_1}{2}, \quad \text{if } l_s < |x| \leq L \text{ for the circumferential part} \tag{11}$$

$$y(x) = \frac{D_1}{2} + \frac{x - l_s}{\tan\left(\frac{\theta}{2}\right)}, \quad \text{if } L_3 < |x| \leq l_s \text{ for the conical part} \tag{12}$$

$$y(x) = -\sqrt{R^2 - x^2} + \frac{D_2}{2} + R, \quad \text{if } 0 < |x| \leq L_3 \text{ for the cylindrical part} \tag{13}$$

Since the analytical solution of Eqn. (13) may be difficult, the function $y(x)$ has been simplified with the following function using the catenary approach.

$$y(x) = \frac{D_2}{2} \cosh(\alpha_b x) \quad \text{if } 0 < |x| \leq L_3 \tag{14}$$

$$\alpha_b = \frac{1}{R \cos\left(\frac{\theta}{2}\right)} \frac{\frac{D_2}{2} + R - R \sin\left(\frac{\theta}{2}\right)}{\frac{D_2}{2}} \tag{15}$$

Finally, the equations have been solved using the proper boundary conditions and final geometry has been verified using FEA.

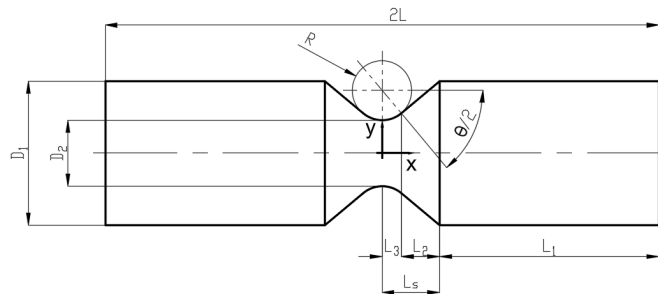


Figure 24: Geometry of notched specimens for the analytical procedure proposed by Dantas et al. [4].

Finally, although Dantas et al. [4] demonstrated the validity of their analytical approach for blunt notch geometries, further analytical methods need to be developed for designing notched specimens with different geometries in ultrasonic fatigue testing of steel.

Models for life prediction of notched specimens in the VHCF regime

The design of notched components subjected to a number of cycles greater than 10^7 cycles has currently some problems that should be addressed in future research. The first one is the limited availability of data in the literature, with the available approaches for assessing the fatigue life and the notch sensitivity validated on a specific material. In this section, the available approaches will be briefly discussed.

Some general indications are given by the ISO standards. Particularly, the EN ISO 1993-1-9 gives some indications about the components subjected to fatigue and produced with structural steels, while the EN ISO 1999-3 is focused on structures made of aluminium. These standards are widely used for components subjected to High Cycle Fatigue (HCF), but they can also be applied to VHCF conditions, as the S-N curves extend up to 10^9 cycles. The procedure proposed by the standards is the following:

- 1) Define the geometry of the component and identify the corresponding detail category in the standards. For example, a plate with a hole is defined by the detail category 140-7 of the standard EN 1999-3.
- 2) Compute the nominal stress $\Delta\sigma$ far from the notch/hole.
- 3) Increase the value of $\Delta\sigma$ by using the value of K_t reported in the plots of the standards.
- 4) Use the S-N curves provided by the standards to evaluate the fatigue life N_f . The different curves represent the detail category selected at point 1. Fig. 25 shows an example of S-N curves digitised from the EN 1999-3

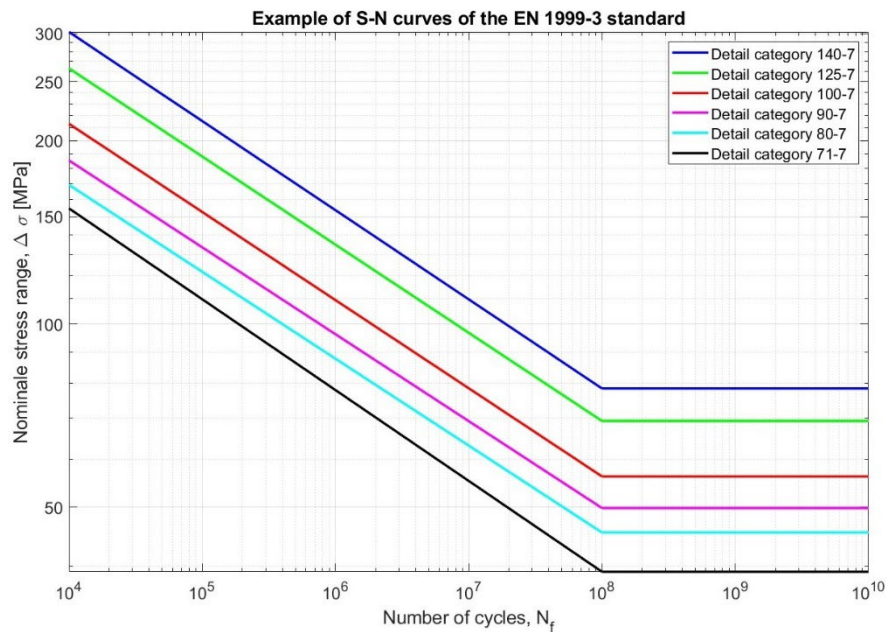


Figure 25: Example of S-N curves given by the EN ISO 1999.

Despite this method being very simple, there are several drawbacks in its application:

- 1) The S-N curves are validated only in the HCF regime, but not in the VHCF regime.
- 2) Only a few geometries (hole and dogbone) are covered by the standards, so it is difficult to apply them to complex structures.
- 3) To obtain the real notch sensitivity, the value of K_t should be integrated with experimental data to compute the value of the notch fatigue factor (i.e. K_f).
- 4) The standards assume that a fatigue limit is present at 10^8 cycles. However, the experimental results reported in this paper have proven that almost all notched specimens do not show a fatigue limit (see also Tab. 6 at column 7).

Another possible approach is based on the use of the notch fatigue factor (i.e. K_f), typical of the HCF fatigue. Particularly, the following steps should be considered:

- 1) Compute the stress concentration factor K_t with the static approach.
- 2) Compute the notch fatigue factor (K_f) using the notch sensitivity (q).

$$K_f = 1 + q(K_t - 1) \quad (16)$$



The values of q can be computed according to Neuber's formulation [30] or Peterson's formulation [31]

3) Compute the number of cycles to failure (N_f) using equation

$$N_f = \left(\frac{\sigma_{nom}^{notched}}{K_f A_0} \right)^{B_0} \tag{17}$$

where A_0 and B_0 are the material constants obtained by interpolation of the S-N curve of the smooth specimens (Basquin formulation), while $\sigma_{nom}^{notched}$ is the nominal stress amplitude applied on the notched specimen.

The advantage of this method is that is very simple. However, there are some problems when applied in the VHCF fatigue:

- 1) The definition of the stress concentration factor is not unique. In fact, it has already been discussed that, in ultrasonic fatigue testing, different authors uses different definitions of K_t .
- 2) The values of q present in the literature [31] are not validated in the VHCF regime.
- 3) The notch sensitivity is not always constant in the VHCF regime, as reported also in column 6 of Tab. 6. As a consequence, for several materials it would not be easy to define a unique value of K_f and q .

Shen et al. [29] defined a Stress Gradient Method (SGM) to apply the Theory of Critical Distance (TCD) [35] also in the VHCF regime. The steps to apply their approach are the following:

- 1) Find a correlation between the number of cycles to failure (N_f) and the critical distance (L). The following substeps are needed:
 - a) Computation of the regularized average stress (η) as the ratio of the axial stress ($\sigma(R)$) to the maximum stress in the critical section (σ_{max}).

$$\eta = \frac{\sigma(R)}{\sigma_{max}} \tag{18}$$

- b) Compute the average stress gradient (χ) as the derivative of η with respect to the radius (R).

$$\chi_{cr} = \left. \frac{d\eta}{dR} \right|_{R=0} \tag{19}$$

- c) Compute the value of the critical radius (R_{crit}) for each number of cycles (N_f), by comparing the average stress computed with the Volume Method ($\sigma_{AV}(R_{crit})$) with the stress of the smooth specimens at the same number of cycles. $\sigma_1(R)$ is the axial stress of the notched specimen at the number of cycles N_f .

$$\sigma_{AV}(R_{cr}) = \frac{3}{2\pi R_{cr}^3} \int_0^\infty \int_{-\pi/2}^{\pi/2} \int_0^{R_{cr}} \sigma_1(r, \theta, \varphi) r^2 \sin \theta dr d\theta d\varphi = \sigma_{nom}^{smooth} \tag{20}$$

- d) Find interpolation constants (A_3 and B_3) in the following equation

$$R_{crit} = A_3 \left(\chi_{cr} N_f \right)_3^B \tag{21}$$

- 2) For a certain value of the nominal stress of the notched specimen ($\sigma_{nom}^{notched}$), compute the critical distance (L) assuming a value for the number of cycles to failure ($N_{assumption}$).

$$L = A_3 \left(\chi_{cr} N_{assumption} \right)_3^B \tag{22}$$

- 3) Use the value of L to compute the averaged stress using the Volume Method (VM).



$$\sigma_{AV}(L) = \frac{3}{2\pi L^3} \int_0^\infty \int_{-\pi/2}^{\pi/2} \int_0^L \sigma_1(r, \theta, \varphi) r^2 \sin \theta dr d\theta d\varphi \quad (23)$$

4) Predict the number of cycles to failure ($N_{prediction}$) using the S-N curves of the smooth specimens.

$$N_{prediction} = \left(\frac{\sigma_{AV}}{A_0} \right)^{\frac{1}{B_0}} \quad (24)$$

5) Verify if the predicted $N_{predicted}$ for the notched specimens is equal to $N_{assumption}$. If this step is verified, the iteration process is ended; otherwise, the value of $N_{assumption}$ is changed and the steps from 2 to 5 are repeated.

In Fig. 26 the flowchart of the process is reported.

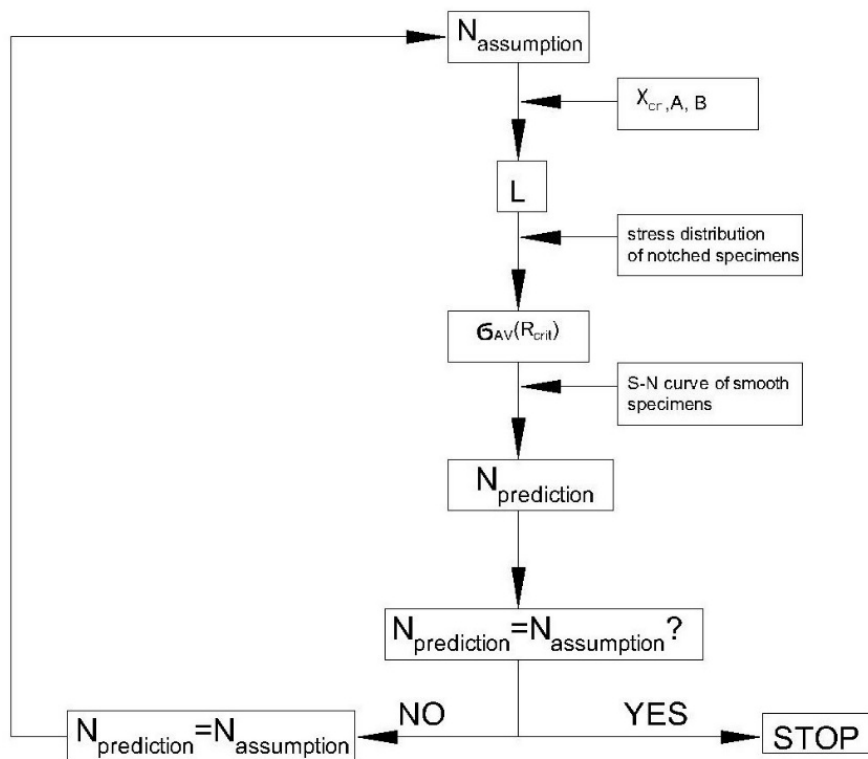


Figure 26: Flowchart of the Stress Gradient Method defined by Shen et al.[29].

According to the Authors, this method can be applied with success to the INCONEL 718 alloy because the data are concerned within ± 3 life factors using their approach. To evaluate the precision of their method, Shen et al. [29] also tried to apply the classical approaches of the TCD introduced by Susmel in the HCF regime [35]. Mechanical Property Method (MPM), Fatigue Testing Method (FTM) and K_t method (KTM). The comparison shows that the SGM of Shen et al. is more precise than the other methods. However, the applicability of their for other materials has not been verified.

Finally, Gao et al. [11] proposed a modification of the Theory of Critical Distance (mTCD). Their idea is to use the Line Method to calibrate the critical distance (l_{LM}^{TCD}) distance at 10^6 cycles by comparing the smooth and notched fatigue strengths. This calibration was already proposed in a previous work in the HCF regime [36]. Then, the following steps are to be followed:

- 1) Use the S-N curve of the smooth specimens to compute the nominal stress of the notched specimens (σ_{nom}^{smooth}) corresponding to a selected number of cycle to failure (N_f).
- 2) Consider a certain value of the nominal stress of the notched specimen ($\sigma_{nom}^{notched}$) and compute the average stress (σ_{eff}) using the Line Method.



$$\sigma_{\text{eff}} = \frac{1}{l_{LM}^{TCD}} \int_0^{l_{LM}^{TCD}} \sigma_1(r, \theta = 0) \varphi(r) dr = \frac{1}{l_{LM}^{TCD}} \int_0^{l_{LM}^{TCD}} \sigma_1(r, \theta = 0) e^{\frac{K_t - 1}{1 + \sqrt{a_N/r}}} dr \quad (25)$$

The equation is different from the classical Line Method of the TCD [35] because Gao et al. introduced the weighting function $\varphi(r)$ which depends on the distance from the notch tip (r), the stress concentration factor (K_t), the notch radius (ρ) and the characteristic length of material defined by Neuber (a_N) [30]. The other terms of the equation are: the principal stress in the critical section (σ_1) and the critical distance (l_{LM}^{TCD}).

- 3) Verify if the effective stress (σ_{eff}) is equal to the nominal stress of the notched specimens ($\sigma_{\text{nom}}^{\text{smooth}}$). If this step is verified, it means that $\sigma_{\text{nom}}^{\text{notched}}$ is the fatigue strength of the notched specimen for the present value of N_f . Otherwise, a different value of $\sigma_{\text{nom}}^{\text{notched}}$ should be selected and the previous steps should be repeated until the step 3 is verified.

The Authors applied this approach to a TC17 and a Ti-8Al-1Mo-1V titanium alloys and they obtained a good correlation between predicted and experimental fatigue strengths, with most of the data falling within the $\pm 5\%$ deviation bands. The accuracy is good and the results are better than the results obtained with the conventional TCD. Despite the authors proved the applicability for two titanium alloys, the authors put in evidence some drawbacks:

- 1) The critical distance has been calibrated at 10^6 cycles, but it is not known if this value is also valid for other materials.
- 2) The method is not based on a physical model.
- 3) Since the weighting function ($\varphi(r)$) depends also on the value of a_N , the applicability of the method is limited to the materials Analysed by Neuber [30].

In conclusion, despite a few approaches in literature to predict the VHCF life of notched components (SGM [29] and mTCD [11]) are available, the applicability of these methods should be verified with different materials. At present, a general valid methodology for the design of parts with notch in the VHCF life range is not available and an experimental validation is always required to ensure a safe design.

Analysis of the results: general trends and differences

In this section, a final comparison of the results obtained by different authors is reported.

Regarding the investigated materials, the number of published articles on steels is eight, while for other metallic materials, there are only a few articles, as shown in Fig. 1. As a consequence, all the following considerations should be validated with a larger number of tests in future works.

The first aspect is that the majority of the authors conducted the fatigue tests at ultrasonic frequency. However, this should not be an issue because almost all the materials are titanium alloys, aluminium alloys and high-strength steels that, according Hong et al. [10], are not sensitive to the loading frequency. The only material whose sensitivity to loading frequency is unclear is the 30C steel, but Fururya et al. [15] proved that the results obtained with ultrasonic testing are comparable to those obtained with low frequency testing.

Regarding the fracture mechanism, almost all the materials are “Type II” and according to Mugharabi [12] have cracks nucleated from internal defects in smooth specimens. However, the last column of Tab. 6 shows that the same materials tested with notched specimens may exhibit cracks nucleated at the surface. The reason for this change in fracture mechanism is still not fully understood and should be investigated in future studies. However, it is probably related to the stress concentration present near the notch tip. Moreover, this phenomenon appears to influence the notch sensitivity in the VHCF regime. Indeed, at column 6 of Tab. 6 it is reported that some materials (SUJ1, EN AW 6082, Ti-8Al-1Mo-1V and TC17) have a notch sensitivity that decreases with the number of cycles. This change may be caused by the different fracture mechanism between smooth and notched specimens. However, this is only a hypothesis because, on the other hand, the S690QL steel shows an increase in the notch sensitivity when the number of cycles increases.

Finally, at columns 7 and 8 the presence of a fatigue limit for smooth and notched specimens is reported. If the material does not exhibit a fatigue limit with the unnotched specimens, the same behaviour is also observed with notched specimens. The 17 Cr2Ni2Mo steel is the only case when the fatigue limit is present only with notched specimens. One possible explanation is, again, the competition between two failure mechanisms (nucleation from internal defects and nucleation from the surface), but the reasons should be analysed in future works.



CONCLUSIONS

The present review of the literature about the notch effect in the VHCF life range leads to the following conclusions:

- 1) The conventional fatigue limit cannot be considered a reliable reference either for unnotched or notched components in the VHCF regime.
- 2) The failure mechanism of notched components in VHCF is not always the same as that observed in smooth specimens. In fact, the stress concentration near the notch can promote surface crack initiation rather than crack initiation from internal defects.
- 3) Notch sensitivity is not necessarily constant in the VHCF regime. In many cases, it decreases as the number of cycles to failure increases.
- 4) The stress concentration induced by notches can be assessed using the static stress concentration factor or the methods proposed by Dantas et al. [4] and Tridello et al. [5] [7]. However, when comparing results from different authors, particular care must be taken in the computation of the notch fatigue factor (K_D).
- 5) Adapted versions of the Theory of Critical Distance are capable of predicting the fatigue life of notched components with limited scatter. In general, all methods available in the literature for modelling notch effect require further experimental validations to prove their validity and that they can be generalised. Nevertheless, these models still require validation through extensive experimental testing. Consequently, a model to predict the fatigue life of notched components still needs to be defined.

To conclude, several results are available in the literature on notch effect, but significant efforts are still to be made to investigate this complex phenomenon. Future research should work on obtaining more experimental data and on developing models accounting for the complex interactions between defects, stress concentration and the microstructure, validated on large experimental datasets and for different materials.

ABBREVIATIONS

The following abbreviations are used in this manuscript:

VHCF	Very High Cycle Fatigue
HCF	High Cycle Fatigue
TCD	Theory of Critical Distance
SEM	Scanning Electron Microscopy
FESEM	Field Emission Scanning Electron Microscopy
EBSD	Electron Backscatter Diffraction

REFERENCES

- [1] Bathias, C. (1999). There is no infinite fatigue life in metallic materials, *Fatigue Fract Eng Mater Struct*, 22(7), pp. 559–565. DOI: <https://doi.org/10.1046/j.1460-2695.1999.00183.x>.
- [2] Bathias, C. (2013). *Front Matter., Fatigue Limit in Metals*, Wiley.
- [3] Sippel, J.P., Kerscher, E. (2020). Properties of the fine granular area and postulated models for its formation during very high cycle fatigue—a review, *Applied Sciences (Switzerland)*, pp. 1–27. DOI: <https://doi.org/10.3390/app10238475>.
- [4] Dantas, R., Gouveia, M., Silva, F.G.A., Fiorentin, F., Correia, J.A.F.O., Lesiuk, G., de Jesus, A. (2023). Notch effect in very high-cycle fatigue behaviour of a structural steel, *Int J Fatigue*, 177. DOI: <https://doi.org/10.1016/j.ijfatigue.2023.107925>.
- [5] Paolino, D.S., Tridello, A., Chiandussi, G., Rossetto, M. (2014). On specimen design for size effect evaluation in ultrasonic gigacycle fatigue testing, *Fatigue Fract Eng Mater Struct*, 37(5), pp. 570–579. DOI: <https://doi.org/10.1111/ffe.12149>.
- [6] Tridello, A., Boursier Niutta, C., Benelli, A., Pagnoncelli, A.P., Rossetto, M., Berto, F., Paolino, D.S. (2024). On the notch sensitivity of as-built Laser Beam Powder Bed–Fused AlSi10Mg specimens subjected to Very High Cycle Fatigue tests at ultrasonic frequency up to 109 cycles, *Fatigue Fract Eng Mater Struct*, 47(11), pp. 4356–4371. DOI: <https://doi.org/10.1111/ffe.14419>.



- [7] Tridello, A., Boursier Niutta, C., Berto, F., Paolino, D.S. (2023). Blunt notch effect on the fatigue response up to 109 cycles of selective laser melting Ti6Al4V specimens, *Fatigue Fract Eng Mater Struct*, 46(9), pp. 3417–3428. DOI: <https://doi.org/10.1111/ffe.14078>.
- [8] Akiniwa, Y., Miyamoto, N., Tsuru, H., Tanaka, K. (2006). Notch effect on fatigue strength reduction of bearing steel in the very high cycle regime, *Int J Fatigue*, 28(11), pp. 1555–1565. DOI: <https://doi.org/10.1016/j.ijfatigue.2005.04.017>.
- [9] Nehila, A., Li, W. (2023). Effect of notch and stress ratio on Very High Cycle Fatigue characteristics of the carburized 17CrNi high-strength steel and life prediction., *Procedia Structural Integrity*, vol. 51, Elsevier B.V., pp. 152–159.
- [10] Qian, G., Hong, Y., Zhou, C. (2010). Investigation of high cycle and Very-High-Cycle Fatigue behaviors for a structural steel with smooth and notched specimens, *Eng Fail Anal*, 17(7–8), pp. 1517–1525. DOI: <https://doi.org/10.1016/j.engfailanal.2010.06.002>.
- [11] Gao, Z., Chen, X., Zhu, S., He, Y., Xu, W. (2023). Notch fatigue behavior of a titanium alloy in the VHCF regime based on a vibration fatigue test, *Int J Fatigue*, 172. DOI: <https://doi.org/10.1016/j.ijfatigue.2023.107608>.
- [12] Mughrabi, H. (2006). Specific features and mechanisms of fatigue in the ultrahigh-cycle regime, *Int J Fatigue*, 28(11), pp. 1501–1508. DOI: <https://doi.org/10.1016/j.ijfatigue.2005.05.018>.
- [13] Hong, Y., Hu, Y., Zhao, A. (2023). Effects of loading frequency on fatigue behavior of metallic materials—A literature review, *Fatigue Fract Eng Mater Struct*, 46(8), pp. 3077–3098. DOI: <https://doi.org/10.1111/ffe.14055>.
- [14] Burkart, K., Bomas, H., Zoch, H.W. (2011). Fatigue of notched case-hardened specimens of steel SAE 5120 in the VHCF regime and application of the weakest-link concept, *Int J Fatigue*, 33(1), pp. 59–68. DOI: <https://doi.org/10.1016/j.ijfatigue.2010.07.006>.
- [15] Furuya, Y., Torizuka, S., Takeuchi, E., Bacher-Höchst, M., Kuntz, M. (2012). Ultrasonic fatigue testing on notched and smooth specimens of ultrafine-grained steel, *Mater Des*, 37, pp. 515–520. DOI: <https://doi.org/10.1016/j.matdes.2012.01.035>.
- [16] Khan, M.K., Liu, Y.J., Wang, Q.Y., Pyoun, Y.S. (2015). Effect of small scale notches on the very high cycle fatigue of AISI 310 stainless steel, *Fatigue Fract Eng Mater Struct*, 38(3), pp. 290–299. DOI: <https://doi.org/10.1111/ffe.12229>.
- [17] Ritz, F., Beck, T. (2017). Influence of mean stress and notches on the very high cycle fatigue behaviour and crack initiation of a low-pressure steam turbine steel, *Fatigue Fract Eng Mater Struct*, 40(11), pp. 1762–1771. DOI: <https://doi.org/10.1111/ffe.12666>.
- [18] Nehila, A., Li, W., Gao, N., Xing, X., Zhao, H., Wang, P., Sakai, T. (2018). Very high cycle fatigue of surface carburized CrNi steel at variable stress ratio: Failure analysis and life prediction, *Int J Fatigue*, 111, pp. 112–123. DOI: <https://doi.org/10.1016/j.ijfatigue.2018.02.006>.
- [19] Schwerdt, D., Pyttel, B., Berger, C. (2011). Fatigue strength and failure mechanisms of wrought aluminium alloys in the VHCF-region considering material and component relevant influencing factors, *Int J Fatigue*, 33(1), pp. 33–41. DOI: <https://doi.org/10.1016/j.ijfatigue.2010.05.008>.
- [20] VDI-Richtlinien: Dusseldorf, G. (2003). VDI. VDI 2230: Systematica Calculation of High Duty Bolted Joints- Joint with One Cylindrical Bolt.
- [21] Cremer, M., Zimmermann, M., Christ, H.J. (2013). High-frequency cyclic testing of welded aluminium alloy joints in the region of very high cycle fatigue (VHCF), *Int J Fatigue*, 57, pp. 120–130. DOI: <https://doi.org/10.1016/j.ijfatigue.2012.10.012>.
- [22] Nie, B., Chen, D., Zhao, Z., Zhang, J., Meng, Y., Gao, G. (2018). Notch effect on the fatigue behavior of a TC21 titanium alloy in very high cycle regime, *Applied Sciences (Switzerland)*, 8(9). DOI: <https://doi.org/10.3390/app8091614>.
- [23] Chapetti, M.D. (2001). Prediction of the fatigue limit of blunt-notched components, 23.
- [24] Yang, K., Zhong, B., Huang, Q., He, C., Huang, Z.Y., Wang, Q., Liu, Y.J. (2018). Stress ratio effect on notched fatigue behavior of a Ti-8Al-1Mo-1V alloy in the very high cycle fatigue regime, *Int J Fatigue*, 116, pp. 80–89. DOI: <https://doi.org/10.1016/j.ijfatigue.2018.05.032>.
- [25] Wang, Q.Y., Bathias, C., Kawagoishi, N., Chen, Q. (2002). Effect of inclusion on subsurface crack initiation and gigacycle fatigue strength, 24.
- [26] Szczepanski, C.J., Jha, S.K., Larsen, J.M., Jones, J.W. (2008). Microstructural influences on very-high-cycle fatigue-crack initiation in Ti-6246, *MEtallurgical and Material Transactions*.
- [27] Liu, X., Sun, C., Hong, Y. (2015). Effects of stress ratio on high-cycle and very-high-cycle fatigue behavior of a Ti-6Al-4V alloy, *Materials Science and Engineering: A*, 622, pp. 228–235. DOI: <https://doi.org/10.1016/j.msea.2014.09.115>.
- [28] Yang, K., He, C., Huang, Q., Huang, Z.Y., Wang, C., Wang, Q., Liu, Y.J., Zhong, B. (2017). Very high cycle fatigue behaviors of a turbine engine blade alloy at various stress ratios, *Int J Fatigue*, 99, pp. 35–43. DOI: <https://doi.org/10.1016/j.ijfatigue.2016.11.032>.



- [29] Shen, J., Fan, H., Zhang, G., Pan, R., Wang, J., Huang, Z. (2022). Influence of the stress gradient at the notch on the critical distance and life prediction in HCF and VHCF, *Int J Fatigue*, 162.
DOI: <https://doi.org/10.1016/j.ijfatigue.2022.107003>.
- [30] Heinz Neuber. (1946). *Theory of Notch Stresses: Principles for Exact Stress Calculation*.
- [31] Peterson R. (1959). *Notch Sensitivity*, McGraw-Hill, *Metal Fatigue*, pp. 293–306.
- [32] Yukitaka Murakami. (2019). *Metal Fatigue: Effects of Small Defects and Nonmetallic Inclusions*, Elsevier: Amsterdam, The Netherlands.
- [33] Bathias, C., Paris P.C. (2004). *Gigacycle Fatigue in Mechanical Practice*, FL, USA, CRC Press: Boca Ranton.
- [34] Tridello, A., Paolino, D.S., Chiandussi, G., Rossetto, M. (2013). Comparison between dog-bone and gaussian specimens for size effect evaluation in gigacycle fatigue, *Frattura Ed Integrita Strutturale*, 26, pp. 49–56.
DOI: <https://doi.org/10.3221/IGF-ESIS.26.06>.
- [35] Susmel, L., Taylor, D. (2007). A novel formulation of the theory of critical distances to estimate lifetime of notched components in the medium-cycle fatigue regime, *Fatigue Fract Eng Mater Struct*, 30(7), pp. 567–581.
DOI: <https://doi.org/10.1111/j.1460-2695.2007.01122.x>.
- [36] Ye, W.L., Zhu, S.P., Niu, X., He, J.C., Correia, J.A.F.O. (2022). Fatigue life prediction of notched components under size effect using critical distance theory, *Theoretical and Applied Fracture Mechanics*, 121.
DOI: <https://doi.org/10.1016/j.tafmec.2022.103519>.